AFRL-ML-WP-TR-2007-4145

QUICK REACTION EVALUATION OF MATERIALS AND PROCESSES

Delivery Order 0010: Bonded Boron Patch Repair Evaluation

Nick J. Jacobs

University of Dayton Research Institute
300 College Park
Dayton, OH 45469-0130

SEPTEMBER 2006

Final Report for 01 March 2005 – 01 September 2006

MATERIALS AND MANUFACTURING DIRECTORATE
AIR FORCE RESEARCH LABORATORY
AIR FORCE MATERIEL COMMAND
WRIGHT-PATTERSON AIR FORCE BASE, OH 45433-7750

NOTICE AND SIGNATURE PAGE

Using Government drawings, specifications, or other data included in this document for any purpose other than Government procurement does not in any way obligate the U.S. Government. The fact that the Government formulated or supplied the drawings, specifications, or other data does not license the holder or any other person or corporation; or convey any rights or permission to manufacture, use, or sell any patented invention that may relate to them.

This report was cleared for public release by the Air Force Research Laboratory Wright Site (AFRL/WS) Public Affairs Office and is available to the general public, including foreign nationals. Copies may be obtained from the Defense Technical Information Center (DTIC) (http://www.dtic.mil).

AFRL-ML-WP-TR-2007-4145 HAS BEEN REVIEWED AND IS APPROVED FOR PUBLICATION IN ACCORDANCE WITH ASSIGNED DISTRIBUTION STATEMENT.

*//Signature//

CAPT. THOMAS NIX
Program Manager
Systems Support Division
Air Force Research Laboratory

//Signature//

EDWARD HERMES, Chief
Acquisition Systems Support Branch
Systems Support Division
Air Force Research Laboratory

//Signature//

GARY A. KEPPLE, Deputy Chief
Systems Support Division
Air Force Research Laboratory

This report is published in the interest of scientific and technical information exchange, and its publication does not constitute the Government's approval or disapproval of its ideas or findings.

*Disseminated copies will show "//signature//" stamped or typed above the signature blocks.

REPORT DOCUMENTATION PAGE

Form Approved
OMB No. 0704-0188

1. REPORT DATE *(DD-MM-YY)*	2. REPORT TYPE	3. DATES COVERED *(From - To)*
September 2006	Final	01 March 2005 – 01 September 2006

4. TITLE AND SUBTITLE
QUICK REACTION EVALUATION OF MATERIALS AND PROCESSES
Delivery Order 0010: Bonded Boron Patch Repair Evaluation

5a. CONTRACT NUMBER
F33615-03-D-5607-0010

5b. GRANT NUMBER

5c. PROGRAM ELEMENT NUMBER
62101F

6. AUTHOR(S)
Nick J. Jacobs

5d. PROJECT NUMBER
4349

5e. TASK NUMBER
S2

5f. WORK UNIT NUMBER
4349S204

7. PERFORMING ORGANIZATION NAME(S) AND ADDRESS(ES)
University of Dayton Research Institute
300 College Park
Dayton, OH 45469-0130

8. PERFORMING ORGANIZATION REPORT NUMBER
UDR-TR-2006-00205

9. SPONSORING/MONITORING AGENCY NAME(S) AND ADDRESS(ES)
Materials and Manufacturing Directorate
Air Force Research Laboratory
Air Force Materiel Command
Wright-Patterson AFB, OH 45433-7750

10. SPONSORING/MONITORING AGENCY ACRONYM(S)
AFRL/MLSC

11. SPONSORING/MONITORING AGENCY REPORT NUMBER(S)
AFRL-ML-WP-TR-2007-4145

12. DISTRIBUTION/AVAILABILITY STATEMENT
Approved for public release; distribution unlimited.

13. SUPPLEMENTARY NOTES
Report contains color content.
PAO Case Number: AFRL/WS 07-1429, 12 Jun 2007.

14. ABSTRACT

The C-141 weep-hole repair, performed in the early 1990s, was the first widespread application of a bonded boron composite repair on a critical structure. This program involved the evaluation of the residual strength and integrity of the bonded boron repairs from aircraft that were decommissioned and to be scrapped. A total of 67 residual strength tests were performed, including 54 original bonded boron composite repaired specimens, 4 new bonded repair specimens, and 9 baseline residual strength specimens. The test specimens consisted of the bonded repair with a substantial amount of the surrounding lower wing structure to allow the specimen to be gripped for testing. A novel Stereo-Optic non-contact surface strain field mapping system was used to characterize the patch/specimen load interaction, strain concentrations at the patch tips, as well as patch delamination events at high stresses.

The results of the project indicate that the bonded boron repair provided significant residual strength after 10 years of accumulated flight time. There appears to be little difference in residual strength of the original repairs as compared to new bonded repairs utilizing the same materials and methods. Of the 54 original repairs tested, a total of nine repairs exhibited some degree of patch failure during the tests, all of which occurred at relatively high stresses.

15. SUBJECT TERMS
C-141 weep-hole, Bonded Boron Repair, Bonded Composite Structural Repair, Residual Strength, Stereo-Optic Strain Measurement, Non-contact Strain Measurement, Strain Field Mapping

16. SECURITY CLASSIFICATION OF:			17. LIMITATION OF ABSTRACT:	18. NUMBER OF PAGES	19a. NAME OF RESPONSIBLE PERSON (Monitor) / 19b. TELEPHONE NUMBER *(Include Area Code)*
a. REPORT	b. ABSTRACT	c. THIS PAGE			
Unclassified	Unclassified	Unclassified	SAR	66	Thomas Nix (937) 656-7213

Standard Form 298 (Rev. 8-98)
Prescribed by ANSI Std. Z39-18

TABLE OF CONTENTS

TABLE OF CONTENTS (Continued)

LIST OF FIGURES

LIST OF FIGURES (Continued)

LIST OF TABLES

PREFACE

This effort was performed under USAF contract F33615-03-D-5607, Delivery Order 0010. The contract monitor during the period of performance was Dr. Edmund Moore of AFRL/MLSC. Mr. James Mazza of AFRL/MLSA (Adhesives, Composites, and Elastomers Group) was the technical director for this effort. All testing and materials characterization work was performed on-site at Air Force Research Lab (AFRL) facilities at Wright-Patterson AFB, Ohio. All mechanical testing was performed at the AFRL/MLSC Mechanical Test Laboratory.

This effort was conducted during the period of March 2005 through September 2006. Other researchers of the University of Dayton Research Institute made significant contributions during the execution of this testing effort and are recognized for doing so. Mr. John Ruschau provided technical input on the test fixture design as well as the details of the test specimen design. Mr. Eric Soppe was the lead mechanical test technician during the execution of the testing and performed the majority of the tests. Mr. Jesse Thumser was the primary machinist tasked with fabrication of test fixtures and test specimens. Mr. Bryan Harris provided finite element analysis models during the grip and specimen design phase of the program.

Additional testing support was provided by Mr. Jack Coate of AFRL/MLSC. Mr. Coate provided test assistance in the form of operation of the Stereo-Optic strain measurement system, post processing of Stereo-Optic data, and specimen preparation for Stereo-Optic measurement. Further assistance with regard to processing and reducing Stereo-Optic strain data was provided by Mr. Josh Deaton, a SOCHE co-op student assigned to AFRL/MLSC.

SECTION 1
INTRODUCTION

In the early 1990's, C-141 aircraft were experiencing structural cracking in the lower integrally stiffened wing skin. This cracking was initiating at cross drilled holes in the riser of the lower wing, referred to as "weep holes" as they allow fuel to transfer between the compartments created by the integral risers of the lower wing skin. A repair method was devised consisting of bonded boron patches adhesively applied to a grit blasted, silane prepped surface. Each bonded boron repair consisted of two patches bonded to the riser in "doubler" configuration on the inside of the wing, and a single OML (outer mold line) patch on the outside surface of the lower wing skin. This repair configuration was utilized for each cracked weep hole that could not be fixed by reaming the hole oversize and cold working. This repair type accounted for over 850 repairs across the C-141 fleet, the majority of which were performed from 1993 to 1995. This bonded composite repair method was also one of the first widespread applications of a composite structural repair on flight critical structure.

After approximately 10 years of service time since the repairs were bonded, the last of the C-141 fleet has been retired. This provided an opportunity to evaluate the properties of the bonded repairs after 10 years of accumulated in-service flight time, including the flight loads and environmental exposure. The overall goal of this program was to evaluate the integrity of the bonded structural repairs via mechanical testing and evaluation of the patch failures. The mechanical testing would consist of residual strength tensile testing to be performed on the patched aircraft wing skins to determine the integrity of the patch, bond line, and surface preparation. To this end, aircraft that were to be scrapped were documented, and rough cut planks containing the bonded repair and surrounding wing skin material were extracted from multiple aircraft. These planks were shipped to Warner Robins ALC for thermography and further tear-down, and then shipped to AFRL for machining and mechanical testing.

There were four primary tasks associated with this test program. The first task was to design and fabricate a set of grips to allow large samples removed from the wing skin containing the integral riser to be tested. The second task was the residual strength testing of 50 repairs that had accumulated 10 years of flight time. The third task involved residual strength testing of a small number of new patches bonded to original aircraft structure to provide a basis for comparison to the original repairs. The fourth task was to test the residual strength of bare planks with unrepaired cracks to provide a lower bound of data to compare repair strength.

SECTION 2
TEST PLAN

The primary tasks performed by UDRI researchers during this test effort are described in the following sections. The design and fabrication details of the grip and test specimens are covered in Section 2.1. Section 2.2 details the test frame and instrumentation that was used in the execution of the residual strength tests. The Stereo-Optic surface strain measurement system is specifically described in detail in this section. Section 2.3 covers the test conditions, loading conditions, and environment in which the tests were performed. Section 2.4 sets forth the specific configurations of the original and new test samples. This includes the primary lot of original repairs that were tested to generate data for a statistical database of 50 repairs, the secondary testing of newly bonded repairs, and the supplemental residual strength tests performed on fatigue cracked unrepaired specimens. Section 2.5 describes the test procedures employed for the residual strength tests. Section 2.6 covers the handling of data as well as data reduction methods and procedures.

2.1 DESIGN OF TEST FIXTURES AND SPECIMENS

2.1.1 Grip Fixture Design

The grips were modeled and designed as a rigid body elements rather than a matched compliance approach taken by WR-ALC on their grips designed for fatigue testing at low loads. The anticipated peak load conditions were based on MMPDS[1] data for 7075 T6 extrusion, using the worst case section dimensions anticipated in the test program.

The grips were designed to allow a range of clamping thicknesses for the skin thickness and riser thickness, as the actual plank dimensions vary considerably across each section and along the length of the plank. The planks as installed on the aircraft are 5 risers wide and approximately 20 feet in length. Three primary planks within the inner lower wing were selected for testing, as they contained the least variability in section dimensions, equivalent loading, and contain a fair amount of repairs. The planks selected for testing were lower inner wing plank number 3, 4, and 5. Each plank has 5 risers, with riser 1 and riser 5 containing a spanwise splice to the adjoining plank. The grip design was then limited to riser 2, 3, and 4 repairs to accommodate the spanwise splice joint. See Figure 1 for an overview of the inside lower wing skin structure.

[1] "Metallic Materials Properties Development and Standardization (MMPDS)", *MMPDS-02*, Federal Aviation Administration, April 2005.

Figure 1. Wing Skin Plank, Denoting Riser Descriptions.

The design incorporated bearing as well as clamping loading to transfer force into the specimen. The original goal of the grip design was to design a grip that would allow reliable failures via bearing load only, as well as clamping load only. However, due to the dimensions of the rough cut panels, and the requirement to make the gage section as wide as possible, this dual loading scheme was unattainable. Best efforts were made to model the bolt pattern to optimize the bearing loads without incurring excessive net area loss. In addition, the fore and aft risers in the grip area were milled with steps to increase shear loading into the skin. This feature helps to introduce load in the outer ends of the specimen, thus helping to reduce load on the highest loaded fasteners nearest to the gage section. Figure 2 displays the front and back side of the lower grip, with a specimen installed and the fixture installed in the test frame.

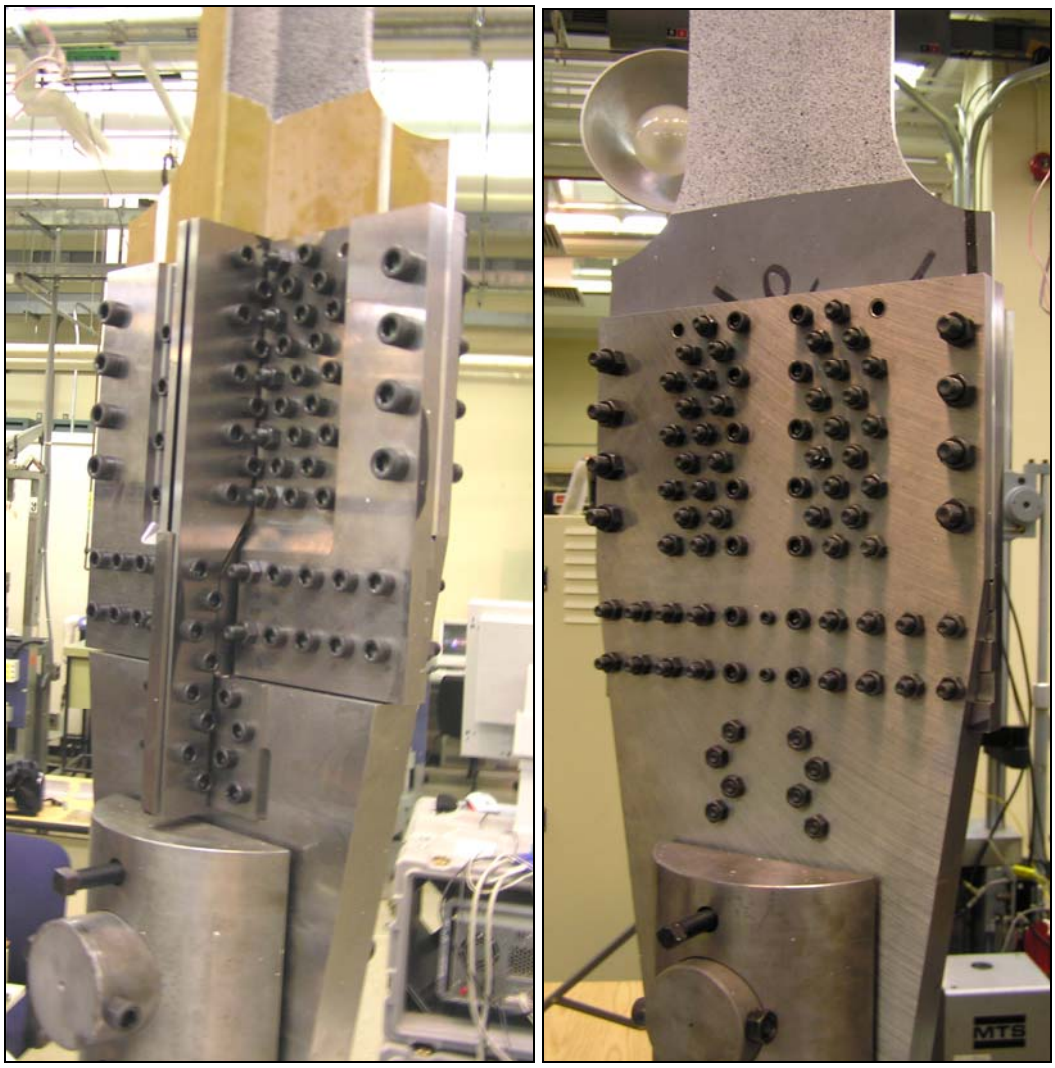

Figure 2. Riser Side (left) and Skin Side (right) Lower Grip Assembly.

The grips were also designed to best accommodate the significant variability within the planks. Within any given length of plank, the specific sections across the width vary widely in thickness and riser height. It was common to see plank cut-outs that had tapering riser height, tapering riser thickness, and varying skin thickness (spanwise as well as lengthwise). This created challenges that required the grip design to be flexible in the range of section dimensions that could be tested. To aid the flexibility, the skin surface was used as a reference surface. All skin thicknesses could then be accommodated by using keyed grip plates that bolt through the specimen and the grip body. The grip plates effectively float above the skin but are rigidly keyed to transfer load regardless of skin thickness of the specimen or taper in the skin thickness. The grip plates are shown in Figure 3.

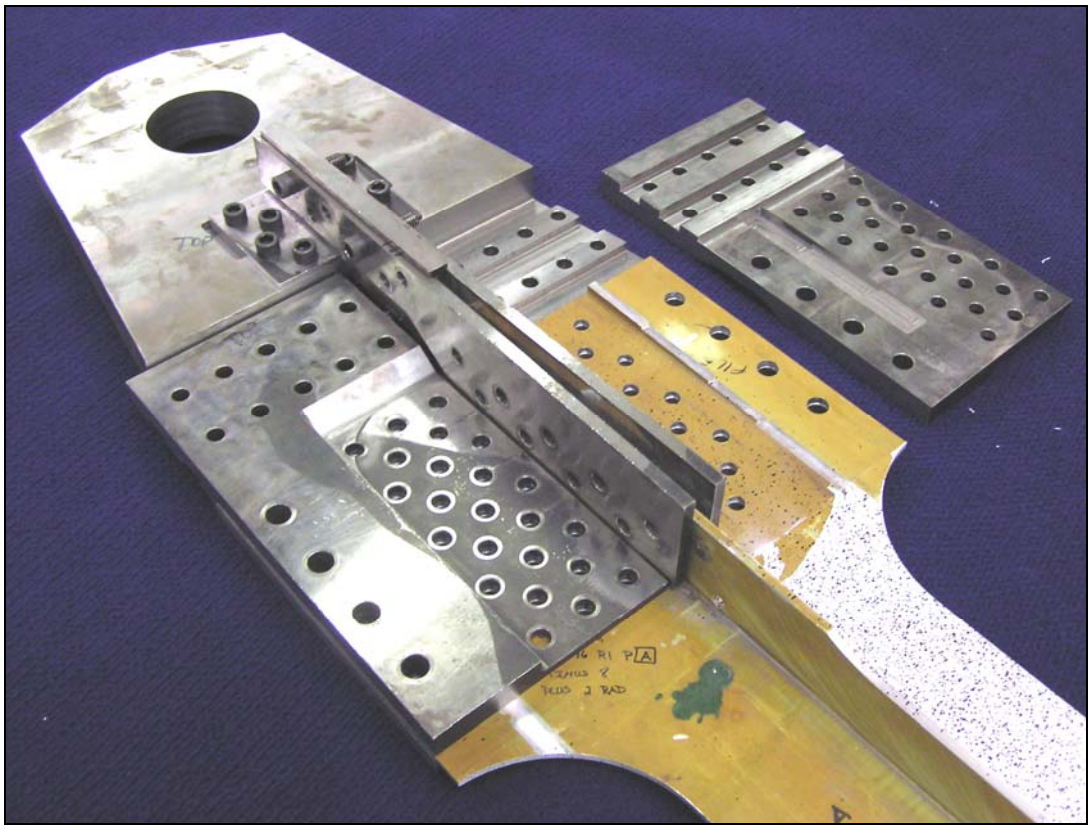

Figure 3. Grip Plates Allowing Varying Skin Thickness.

The riser grip plates employ a similar keyed and bolted arrangement to accommodate a variety of riser thicknesses. Because the plates are separate and open to the top, varying riser heights can be accommodated. As stated previously, the skin surface was used as the reference surface. The vertical location of the riser bolt array was based on this reference plane, eliminating the need to allow the riser grip plates to change position in the vertical plane to accommodate a taller or shorter riser. See Figure 4 for a picture of the riser grip plates.

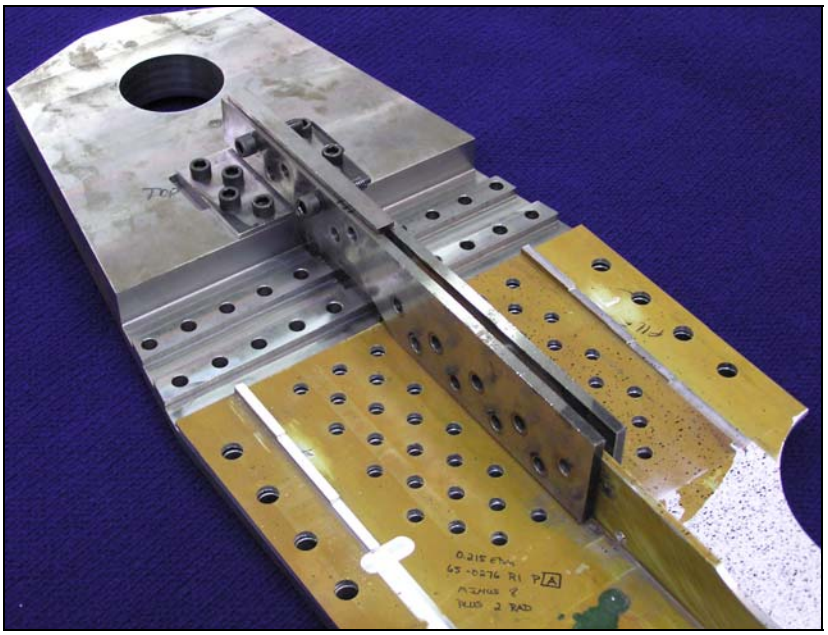

Figure 4. Riser Grip Plates For Varying Riser Height and Thickness.

Due to the configuration of Riser 4 repairs, an additional set of grip plates were manufactured. The plank area adjacent to Riser 5 is the spanwise splice joint, consisting of a row of fasteners atop of a raised rib to create a lap joint with the adjacent plank (Riser 1 on the adjacent plank). Due to the hole pattern already present interfering with the grip bolt array, the spanwise splice and Riser 5 were milled across the thickness, creating additional bearing surface and shear area. Modified grip plates for this configuration were manufactured to accommodate the increased width of the steps. See Figure 5 for a picture of a Riser 4 specimen with the modified grip plate laid over to show the modified pocket.

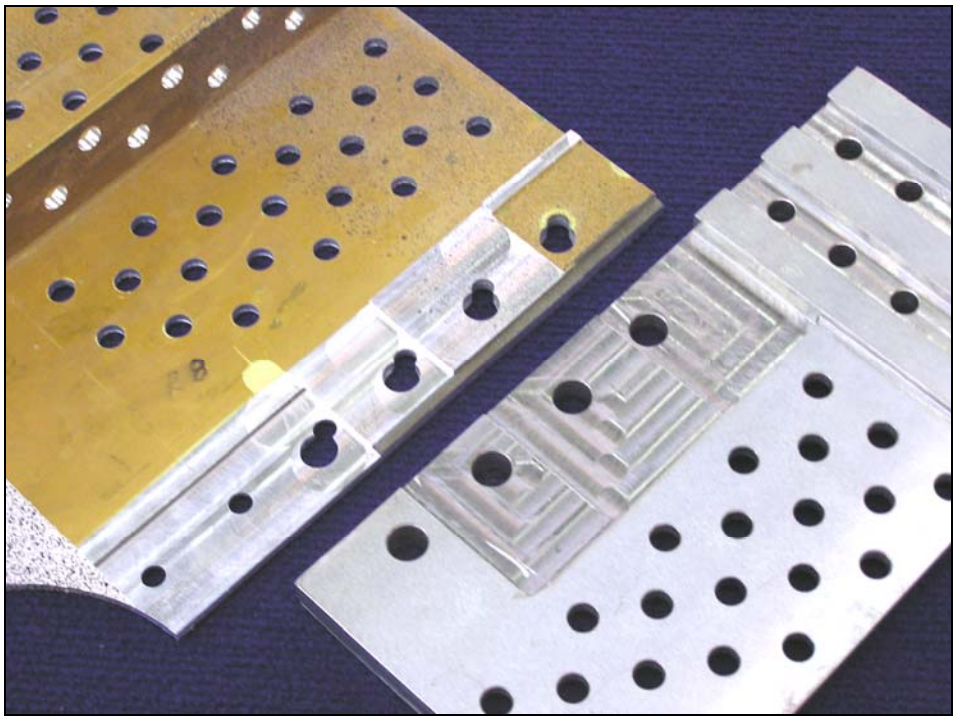

Figure 5. Riser 4 Specimen with Modified Grip Plate.

2.1.2 Specimen Design

The initial specimen design was a dogbone-shaped coupon design that was scaled up to accommodate the maximum permissible width and length. This was intended to test the patch with the most possible area of aluminum substrate around it, to simulate the actual loading of the plank as if it was in the aircraft. However, this gage section width was reduced to 6.5 inches due to test machine capacity limitations as well as reductions in the effective loading in the grip. The overall length of the specimen was also limited by machine physical capacity. The grip area was approximately 12 inches in length from the blend radius to the end of the specimen. The blend radius was designed with a 3-inch radius to maximize the grip area without causing excessive stress concentration at the tangent of the blend radius to the gage section. The bolt array matches that of the grip, which is a compromise between maximizing the bearing area while retaining sufficient net area between the fasteners under the grip. Steps were milled into the adjacent risers on each side of the repaired riser to create more bearing area. The steps lock into pockets milled into the grip plates. A picture of an example 24-inch gage length specimen (48-inch overall length) is detailed in Figure 6.

Figure 6. Example Specimen of 24-Inch Gage Length Design.

The specimen location within the plank was dictated by the location of the weep holes in the length of the rough cut plank. In general, there were two weep holes that fall in the gage section, one each falling near or in the grip area. One of the two weep holes in the gage section was always the repair. When tested, this configuration would consistently fail through the unrepaired weep hole. This configuration also required the repair to be offset from the center of the specimen, primarily to accommodate the one of the unrepaired weep holes in the grip hole pattern. There were some early tests where failures initiated due to a weep hole falling too close to the grip bolt array, breaking through the weep hole, into the grip area, and into the blend radius. Offsetting the patch from the center of the specimen was not desired, but had to be done to accommodate the unrepaired weep holes. There was also concern that if the patch tips were too close to the blend radius, "far field" loading conditions could not be assured. To alleviate this concern, the specimen was placed in the plank such that the closest edge of any repair was 4 inches or more from the tangent of the blend radius. The Stereo-Optic (SO) results were examined to confirm that this configuration produced acceptable strain field distribution for any suspect specimens.

To alleviate some of the geometry induced problems, alternative specimen designs were produced. The 24-inch gage length specimen was modified slightly to produce a 22-inch and a 20-inch gage length version. These designs allowed alternative specimen placement within the plank when the planks were initially laid out for machining, eliminating much of the geometrical problems with hole spacing, holes near the end of the gage section, and holes in unfavorable locations in the grip section.

The early test results were positive, but it was desired to introduce more load into the specimen (and therefore the patch repair). It was decided that the best method to accomplish this would be a specimen that allowed the unrepaired weep holes to be placed in the blend radius. The specimen was redesigned to accommodate the most common weep hole spacing, approximately 12 inches on center, to allow the unrepaired weep holes to be placed in the blend

radius. This provided a gage section that was of continuous cross section with the only exception of rib clip holes. The rib clip holes are small, approximately 0.180-inch in diameter, compared to a typical weep hole of 0.284-inch diameter or larger.

The revised specimen was designed to allow only one weep hole in the gage section, which was the repaired weep hole. The inboard and outboard adjacent weep holes would then fall safely into the blend radius in the revised design. The revised design utilized an 18-inch gage length, with an overall length of 40 inches. This design also eliminated the occurrence of weep holes in the grip area, reducing the number of potential failures in the grip. The only remaining holes in the gage section were rib clip holes, which are much smaller in diameter (0.185-inch diameter compared to typical weep hole at 0.284-inch diameter) and did not cause significant problems. This configuration also allowed the repair to be centered in the gage length of the specimen. See Figure 7 for a picture of a typical 18-inch gage length specimen. Note that the unrepaired weep holes fall in the blend radii, causing no interference with the gage section.

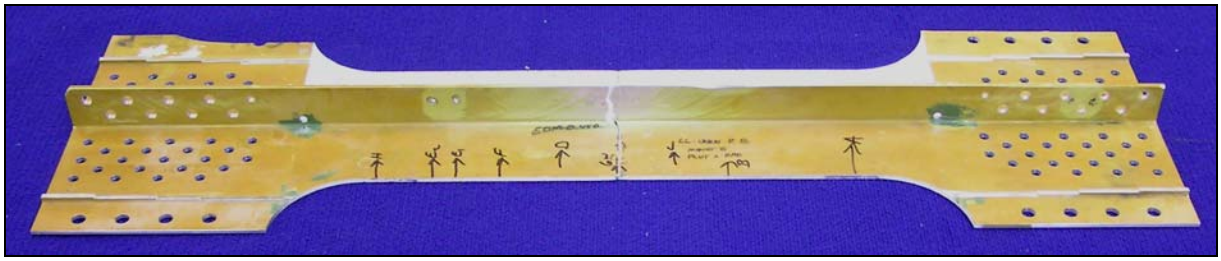

Figure 7. Revised Specimen Design with an 18-Inch Gage Length.

The milling of the risers adjacent to the test section riser was performed on all specimens. This feature allowed load to be introduced without creating additional load on the fasteners, especially the critical fasteners on the first row. These milled steps, along with the accompanying pockets milled into the grip plates, are shown in Figure 8.

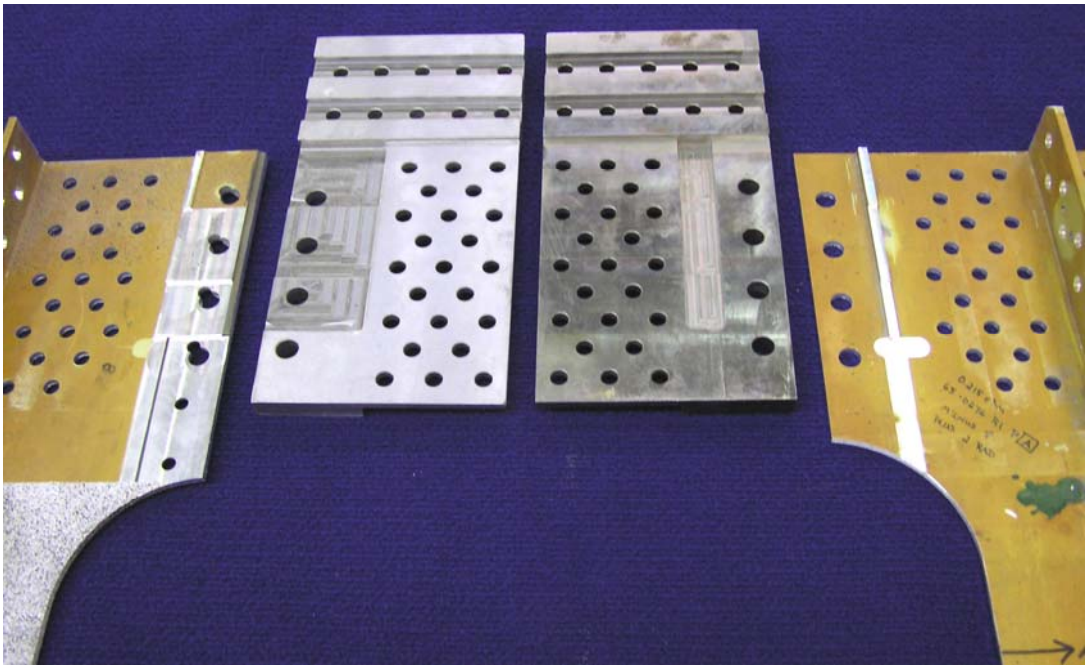

Figure 8. Riser 4 Modified Grip Plates and Specimen (Left) as Compared to Standard Configuration (Right).

2.2 TEST SETUP

2.2.1 Test Frame

A servo-hydraulic test frame of 200 kip capacity was used in the execution of the residual strength tests as shown in Figure 9. All tests were performed in constant rate displacement control mode of 1.2 inches per minute.

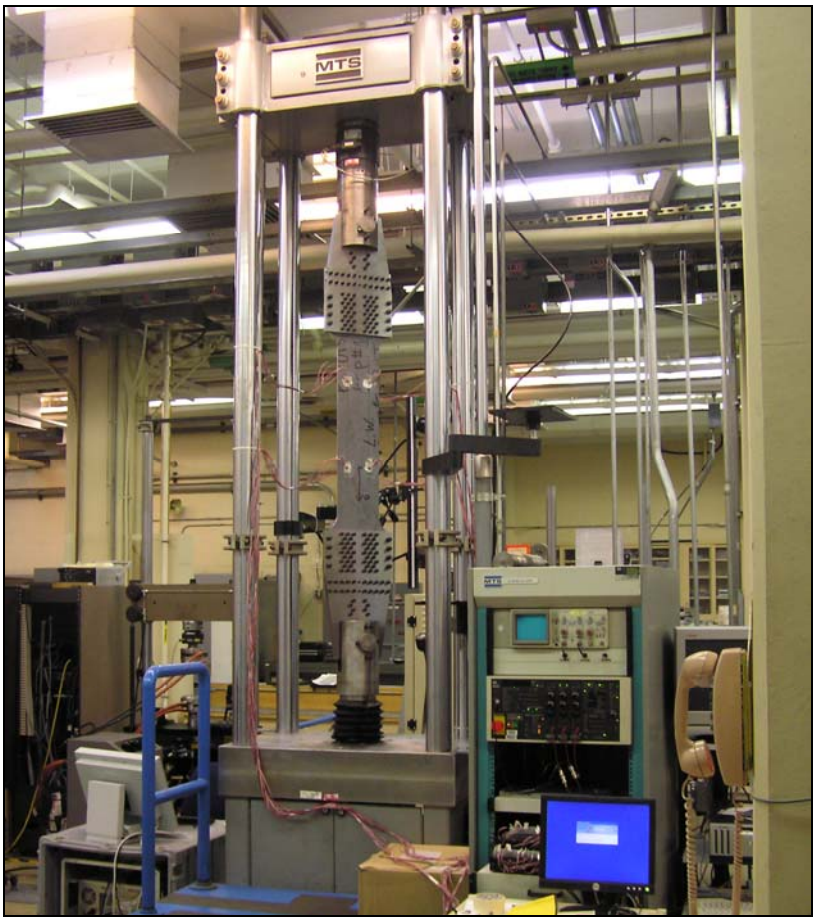

Figure 9. 200 kip Servo-Hydraulic Test Frame.

2.2.2 Strain Data and Analog Signal Acquisition

All strain data, as well as high level analog signals for the load and displacement channels, were recorded with a National Instruments modular SCC (Signal Conditioning, Compact) data acquisition system. This system utilized a LabVIEW data acquisition program that was custom written and configured for this project. Up to 32 channels of mixed signal data were acquired for each test. Each strain channel was individually calibrated and/or verified in place using a calibrated decade resistance box. Strain gage locations varied depending on the specific group of the specimen (initial 10 specimens, remaining repair specimens, or sharp crack residual strength specimens). In general, the earliest tests utilized several strain gages. As testing progressed and the results continually indicated that alignment was well under the goal limit values, the number of strain gages per specimen was reduced throughout the matrix. However, in all cases, 2 rosette gages (3 elements at 0°, 45°, 90°) were used on the riser patch on each specimen. Riser patch gages were located at the midplane of the patch at 1/3 and 2/3 length of the patch in the longitudinal direction.

2.2.3 Stereo-Optic System

A novel strain measurement device was utilized in this project, referred to as a Stereo-Optic (SO) strain measurement system. The system is a GOM Optical Measuring Technologies optical test system. It uses ARAMIS 3D Image Correlation software, version 5.4.1, also manufactured by GOM. The system is exclusively marketed and sold in the United States by Trilion Optical Test Systems of West Conshohocken, PA. The SO system was configured to acquire images and analog load data simultaneously at a rate of 1 Hz during each test. The cameras used are four megapixel grayscale GOM cameras, using 2.8/20mm lenses.

The SO system measures surface strain by acquiring digital images of a 2D or 3D surface that has been "speckle" painted. Generally this speckle paint is applied with flat black paint overspray over flat white background paint. Sample images used for calculation are displayed as Figure 10.

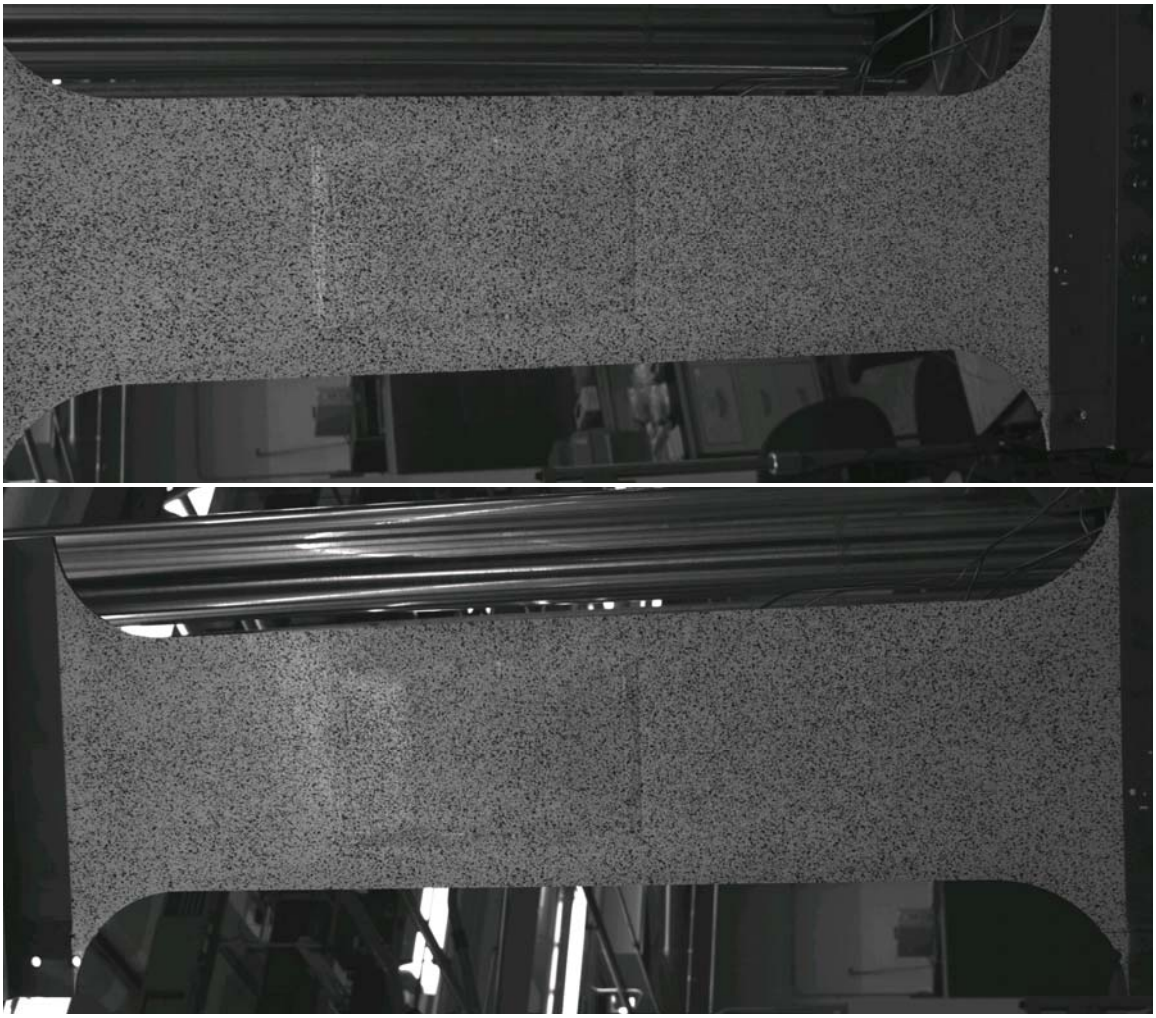

Figure 10. Left (Top) and Right (Bottom) SO Images of OML Patch.

These images are then processed for “correlation” or mapping the individual speckles relative to each other. These maps are combined from both left and right images to form a point cloud of any 3D surface within the field of view and the depth of focus. This pair of images, acquired simultaneously, is referred to as a stage. The stage is assigned a number for later reference. Figure 11 shows the same images referenced above, with an overlay of the “correlated” point cloud. Note the edge regions have trouble correlating (not completely green), as the system is attempting to reference the edge of the specimen as a point.

Figure 11. Left (Top) and Right (Bottom) Correlated SO Images.

The images are then post processed which combines the individual stages acquired during the test, and compares the relative position of each speckle to the corresponding speckle position from other stages. The most important comparison is the relative position of each speckle to that of the baseline stage (no load stage). Once the processing is completed, a map of relative displacements can be made, which provides a strain map of the surface of the point cloud. The strain can be displayed in a number of ways, both dependent and independent of the coordinate

system origin and direction that is designated by the operator. An example of the post processed strain map is overlaid on the original left image in Figure 12 below.

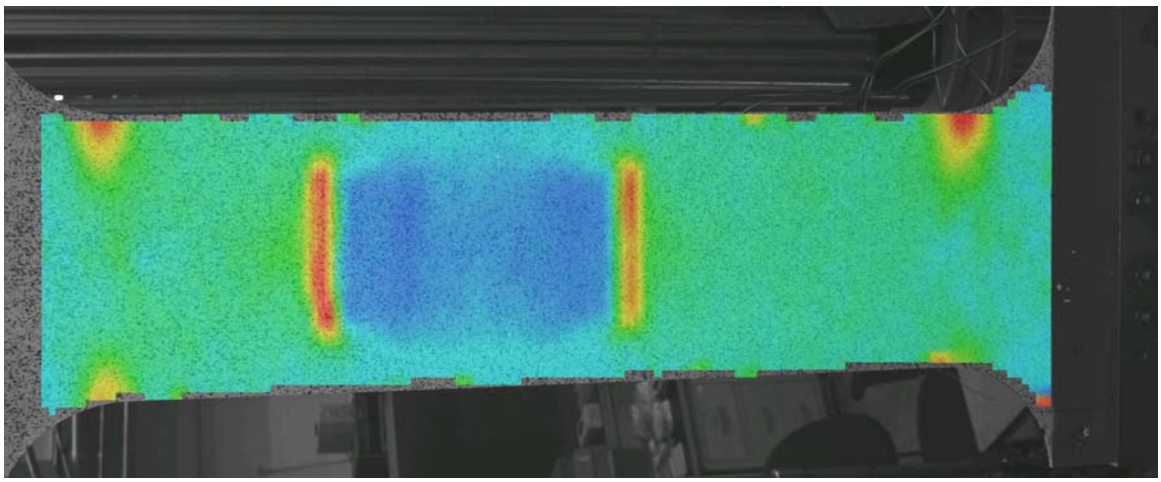

Figure 12. Left (Top) Image with SO Strain Map Overlayed.

This post processed strain map is generally displayed alone as a composite image. The overlay in Figure 12 is provided for understanding, but the general calculated strain "map" is one image per stage. Figure 13 is the same strain map referenced above as a stand-alone image. The bonded boron OML patch is clearly visible in the center of the image, denoted by the low (blue color) strain detected on the surface due to the increased stiffness of the patch in comparison to the aluminum substrate surrounding it.

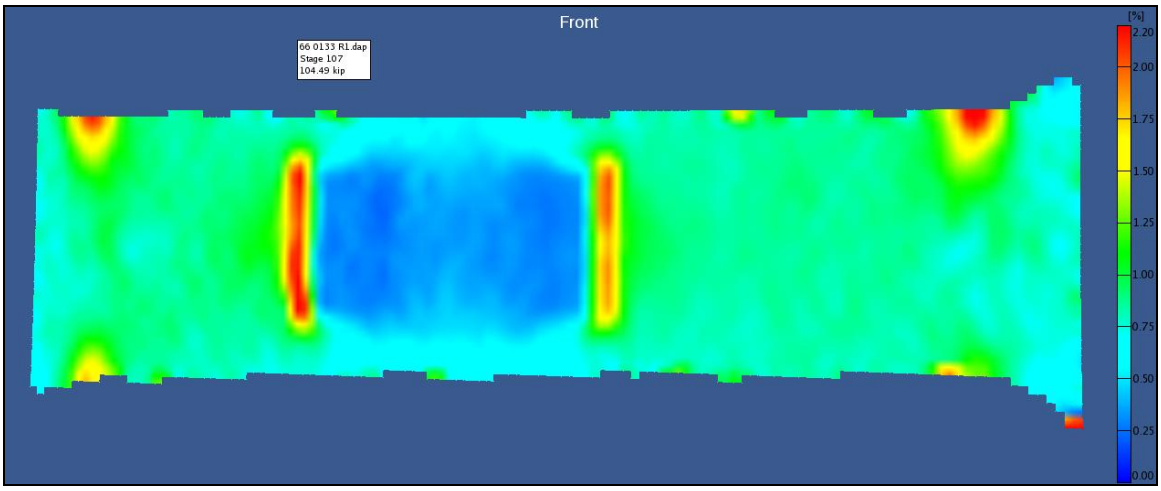

Figure 13. Strain Map Generated by SO System.

The SO system is also capable of measuring out-of-plane displacements and strain associated with those displacements. By measuring the speckle movement toward and away from the cameras, this displacement can be measured and plotted. This information was helpful

for alignment purposes and identification of patch events if the load path was changed by the event.

Significant effort was made to correlate the SO strain data with the strain gage data, to verify the results of the SO system as well as to instill confidence in the measurement technique. This verification was done with one of two techniques. The first technique involved strain gaging a specimen, then speckle painting the specimen in all other areas. This method provides strain information from the same face for comparison, but a SO measurement cannot be made at the exact gage location. The best that can be done is to infer local SO measurements around the gage are the same as under the gage, then compare. An example of this is shown in Figure 14 with the obvious drawbacks, as each strain gage wire and the pieces of cellophane tape to hold the wires cause problems in the local area of the SO measurement.

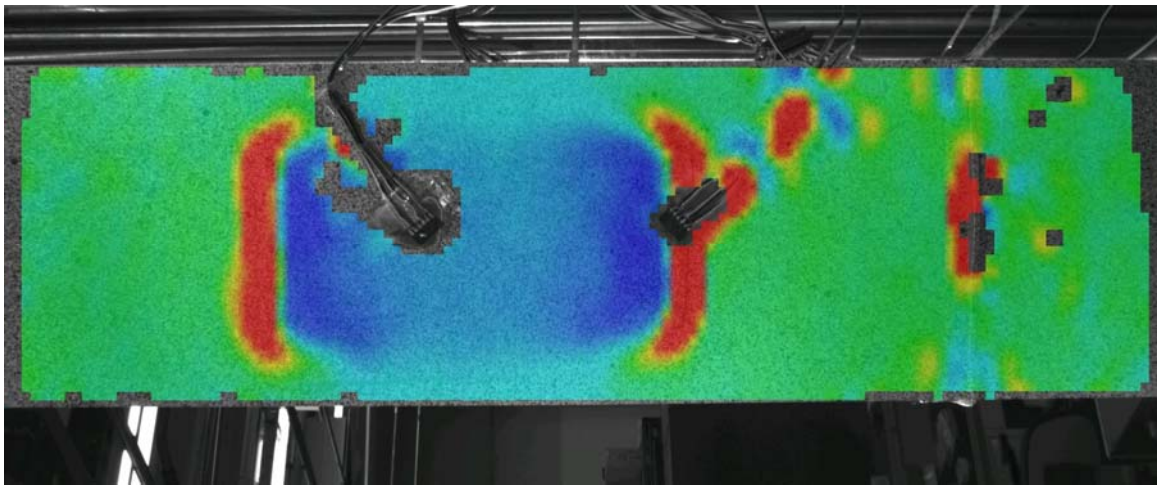

Figure 14. Strain Gage/SO Verification Specimen Overlay.

The second verification technique was the use of a backside strain gage, comparing the two measurements taken on the front and back. This assumes that the front and backside of the specimen experience the same strain, which is not necessarily true. Care was taken to pick verification locations that were well away from edges, stress concentrations, risers, patches, holes, weep hole skin reinforcement pads, and other features.

Both techniques confirmed that the SO system is extremely accurate when there is significant amount of strain and load in the specimen (more than 5% of expected ultimate load). For very small strains experienced at low loads (under 5%), the SO system lacked sufficient resolution. This is due primarily to the lack of clearly detectable movement of individual speckles, and secondarily as an artifact of the large standoff distance required to get the entire gage section of the specimen within the SO measurement window (less pixels per individual

speckle). Figure 15 contains a graph illustrating this accuracy and correlation between strain gage data and data obtained from the SO system. The gage location illustrated in this comparison is on the skin surface of the riser side; the SO data point is on the backside of the gage location (in the identical area of the skin on the OML side of the specimen). The maximum strain deviation (difference in gage strain versus SO strain) at any given load is approximately 200 microstrain (0.02% strain).

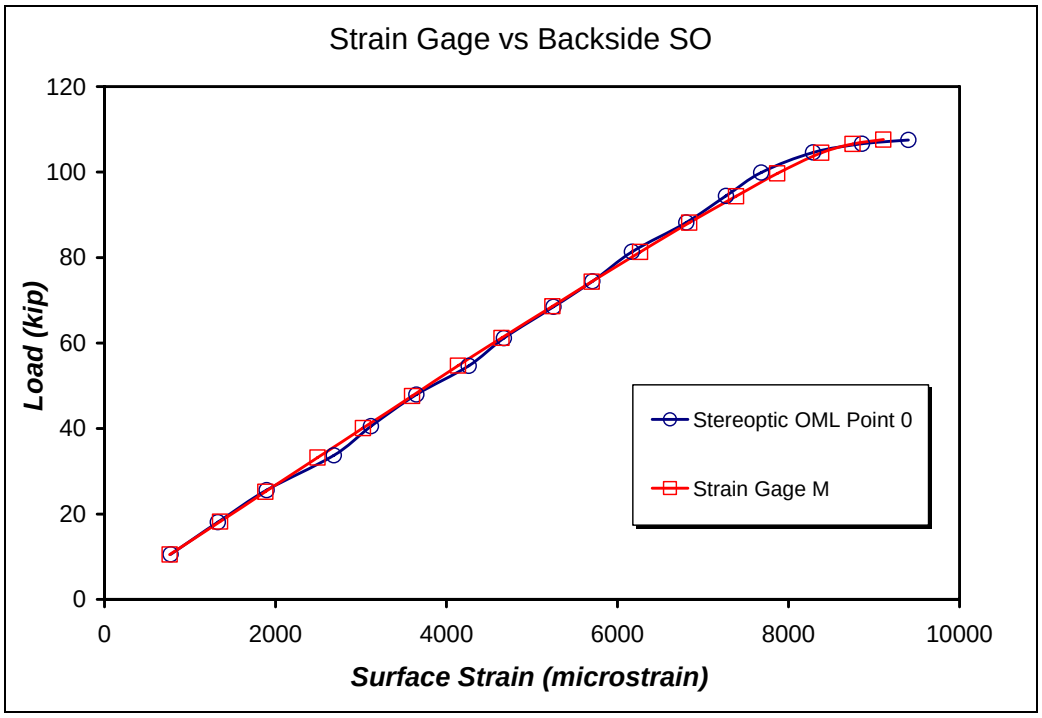

Figure 15. Correlation of Strain Gage and SO Data.

2.3 TEST CONDITIONS

2.3.1 Test Environment

All tests were conducted at room temperature in a laboratory air environment. No conditioning was performed on the specimens. All specimens were stored in a room temperature non-condensing environment at all times after receipt at AFRL. It should be noted that the rough cut planks were stored outside at Warner-Robins AFB, Georgia, prior to being shipped to AFRL for machining. The rough cut planks were shipped on an open pallet. Upon receipt of the planks, some condensed moisture was present in the foam packing material. It should be noted that the planks received would not have been tested sooner than 2 weeks after receipt to account for specimen layout, machining time, and test prep time. In all cases, the fiberglass layers, as well as the paint and sealant, were intact on all patches.

2.3.2 Strain Rate

All tests were conducted in displacement control at a constant rate of displacement at 1.2 inches per minute, corresponding to a minimum strain rate of 0.050 inches/minute per inch of specimen gage length. This displacement rate was sufficient to satisfy the loading rate and strain rate conditions recommended in ASTM E 8[2] for all specimen designs.

2.3.3 Alignment

A significant effort was made to measure and improve specimen alignment during the beginning of the test program. ASTM E 8, the standard for tensile testing of metallic materials, does not provide specific guidance for maximum allowable bending; it simply states that excessive bending adversely affects the results of the test, and efforts should be made to minimize bending. ASTM E 466[3], the standard for fatigue testing of metallic materials, provides a maximum bending value of 5%. Fatigue tests are much more sensitive to bending effects compared to tension tests (for ductile metallic materials); therefore, a self-imposed goal of 10% maximum bending was used as a guideline. Due to the nature of the cross section and the overall scale of the specimen, there was little that could be done to artificially force the specimen into perfect alignment via conventional methods. This problem is compounded when the patch is considered, as the increased stiffness of the patch is applied in an unbalanced manner across the length of the specimen.

The specimens were loaded to approximately 20% of the expected ultimate load for the alignment check. During alignment and alignment verification activities, multiple points taken across multiple cross sections were interrogated to determine bending in multiple planes. The strain gage readings were compared to the SO results for the same areas of the skin (or opposite side as appropriate) along multiple planes to determine bending.

After initial alignment activities and optimization, bending strains were generally held to 7 to 8% or lower. Figure 16 illustrates a typical surface strain response after a complete residual strength test, plotted for multiple locations of strain gage as well as SO data. The strain gage and SO measurement points for this graph were placed back to back and side to side along a single cross section.

[2] "Standard Test Methods for Tension Testing of Metallic Materials", ASTM E 8, American Society for Testing and Materials, revised 2001.
[3] "Standard Practice for Conducting Force Conrolled Constant Amplitude Axial Fatigue Tests of Metallic Materials", ASTM E 466, American Society for Testing and Materials, revised 2001.

Subsequent tests continued to follow the same alignment procedures. The specimens were always instrumented with a minimum of two rosettes on the riser patch, both placed on the unspeckled riser patch. The linear elements of each rosette, located at 1/3 and 2/3 position along the patch length, were used for comparison to the SO data on the opposite side riser patch. The SO results (strain and out of plane displacement) recorded for each subsequent test indicated that alignment continued to be a non-issue.

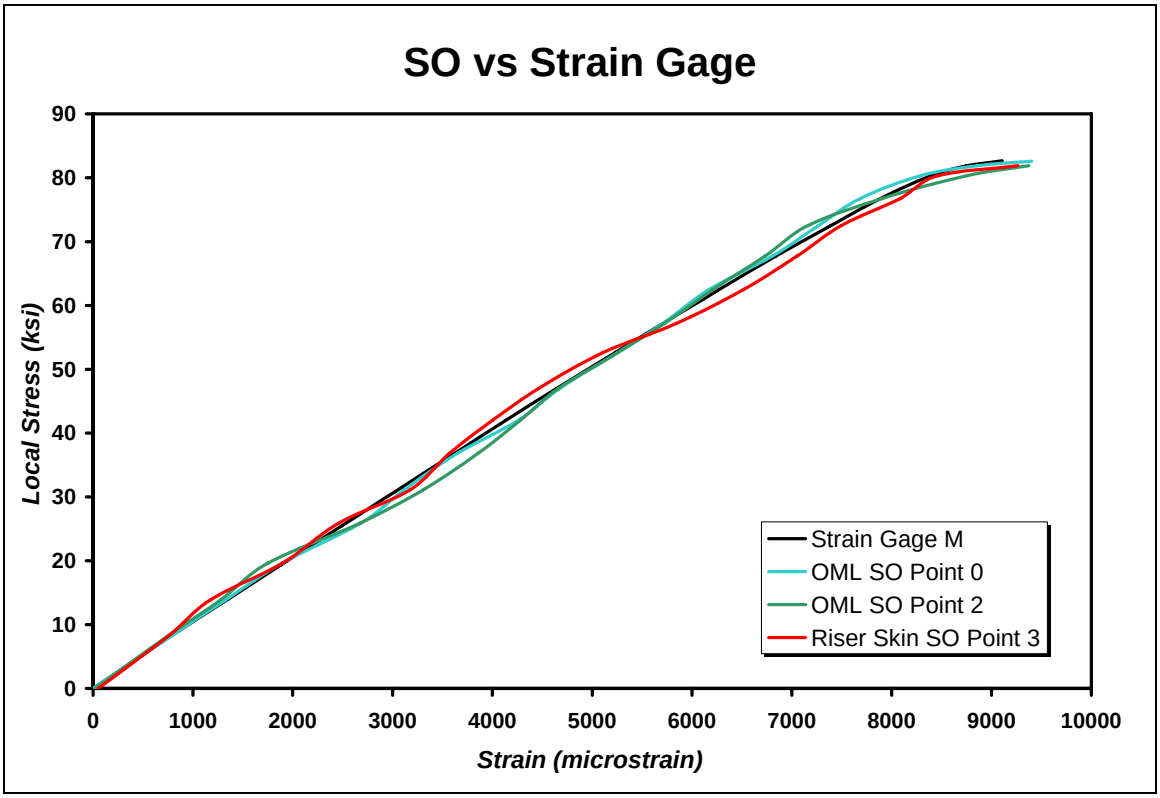

Figure 16. Typical Mixed Signal Strain Response with Acceptable Alignment.

2.4 TEST SAMPLES

2.4.1 Original Repair Patch Configurations

The original repairs were performed by four primary contractors. Each contractor used a different repair design until the repairs were standardized later in the effort. The original repairs tested were a mix of all four repair types. The repair contractors included Lockheed Martin (LM), Warner Robins ALC - Technology and Industrial Support Directorate (TI), Composite Technology Incorporated (CTI), and Chrysler Technologies Airborne Systems (CTAS). The primary repair designs consisted of square edge patches and octagonal patches (clipped edge).

Both of these designs were bonded to the lower wing skin in two directions: aligned with the riser, and angled approximately 20° off the riser centerline to coincide with the primary loading direction of the lower wing skin. In all cases, the riser patch design followed the OML patch design in terms of clipped or square edge patches. Figures 17 through 20 detail the variety of patch designs tested. Table 1 details the patch data specific to each original repair that was selected for residual strength testing. The table covers the patch design, original repair contractor, and crack length and direction information for each repair.

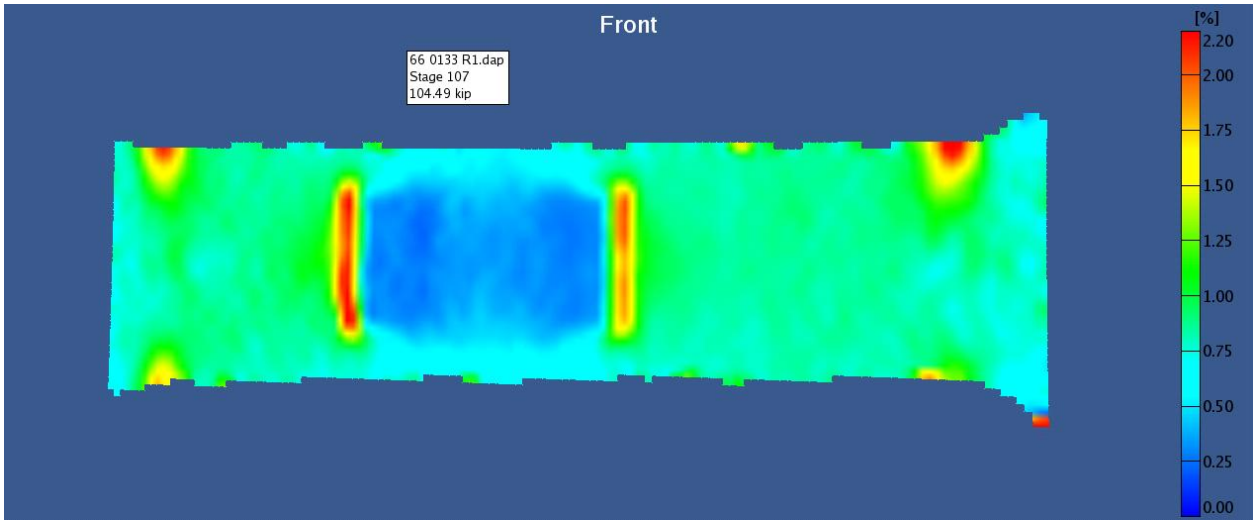

Figure 17. Original Patch Design - Aligned Square Edge Patch.

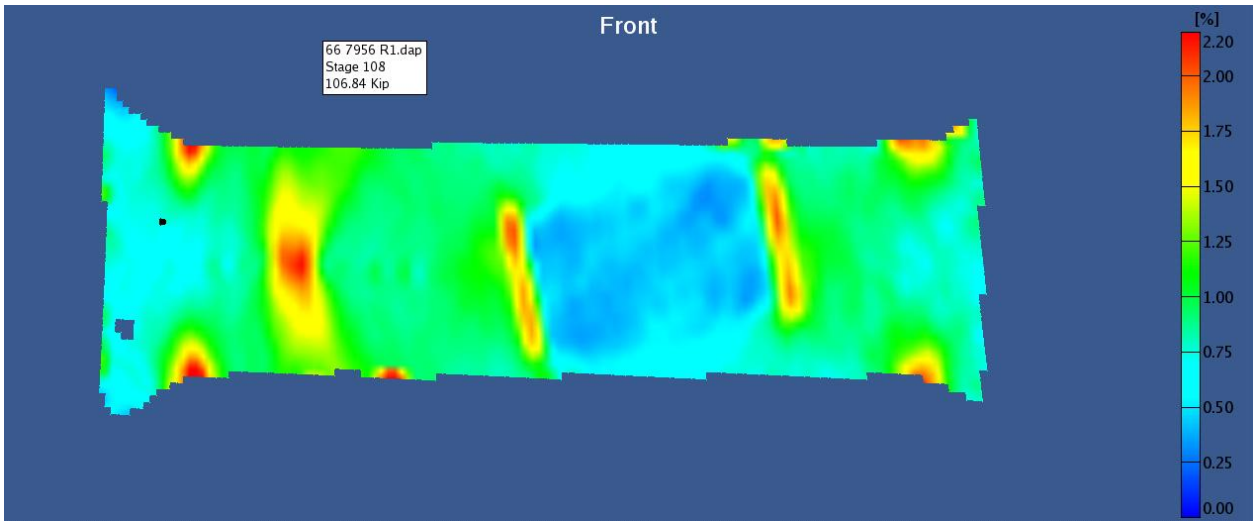

Figure 18. Original Patch Design -Angled Square Edge Patch.

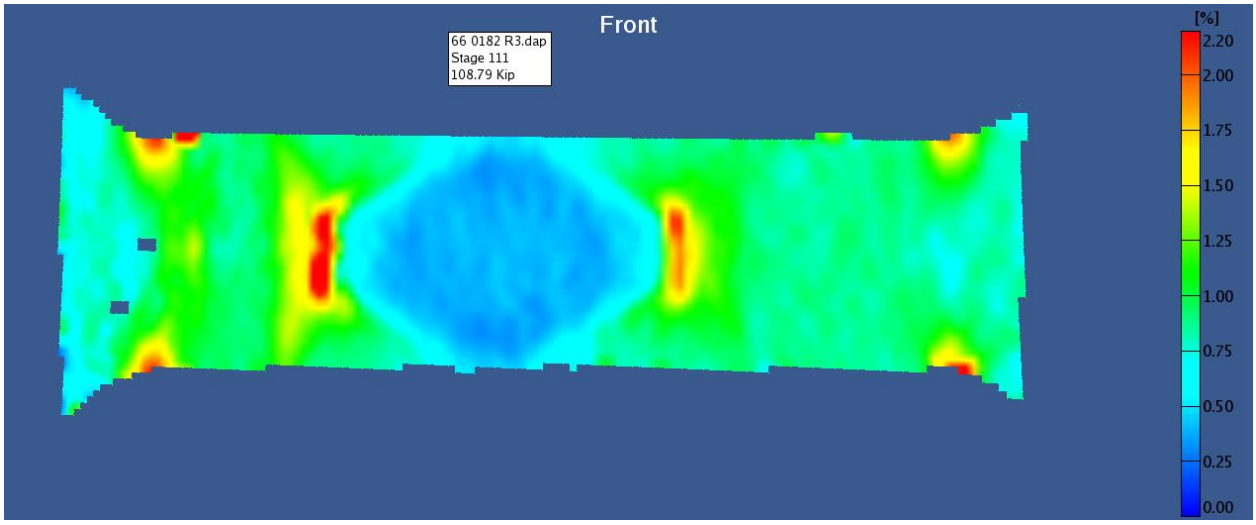

Figure 19. Original Patch Design - Aligned Clipped Edge Patch.

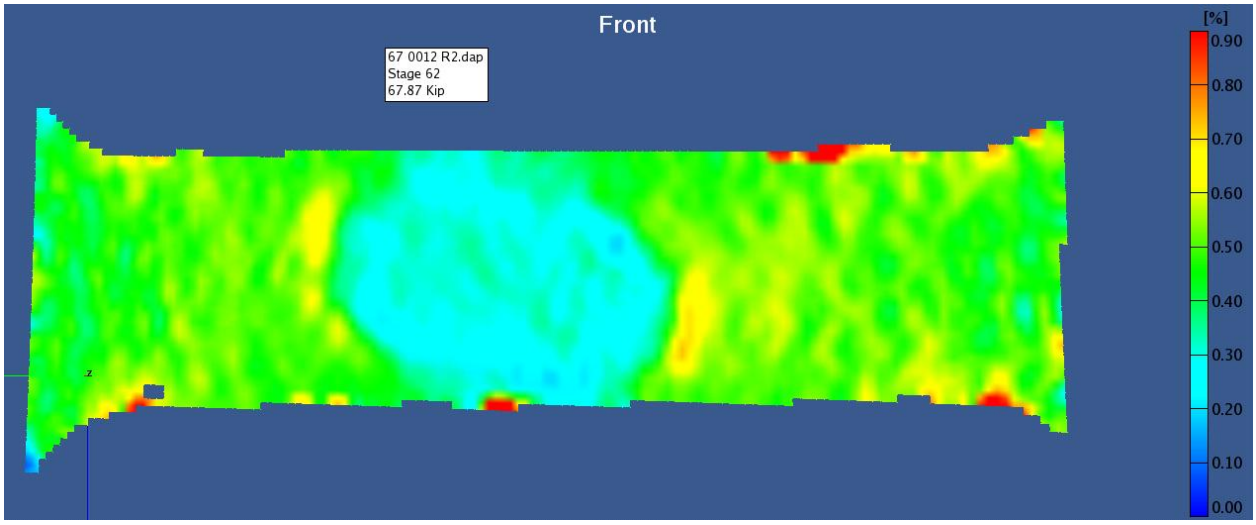

Figure 20. Original Patch Design - Angled Clipped Edge Patch.

Table 1. Original Repairs – Patch Configuration, Crack Length and Orientation

Test Number	Specimen (Repair) Number	Test Date	Gage Length	Patch Design	Patch Axial Orientation to Riser	Patch OEM	Crack Length	Crack Direction
1	66-0156 R 1	11/21/2005	24	Rounded Corner	Aligned	LM	0.625	Up
2	66-0209 R 8	3/3/2006	24	Square Edge	Aligned	TI	0.125	Down
3	64-0643 R 9	3/8/2006	24	Clipped Edge	Aligned	TI	0.06	Up
4	64-0643 R 8	3/17/2006	24	Clipped Edge	Aligned	TI	0.06	Up
5	66-0199 R 1	3/20/2006	24	Clipped Edge	Aligned	TI	0.03	Up
6	66-7955 R 2	3/23/2006	24	Square Edge	Angled	CTI	0.25	Up
7	65-0245 R 2	3/24/2006	24	Clipped Edge	Aligned	TI	0.03	Down
8	66-0168 R 1	4/6/2006	24	Clipped Edge	Aligned	TI	0.25	Down
9	66-0209 R 9	4/10/2006	24	Square Edge	Aligned	TI	0.125	Down
10	64-0643 R 5	4/11/2006	24	Clipped Edge	Aligned	TI	0.06	Up
11	64-0612 R 2	4/12/2006	24	Square Edge	Aligned	TI	0.0625	Down
12	66-0153 R 1	4/13/2006	24	Square Edge	Aligned	CTI	**	Down
13	67-0016 R 5	4/13/2006	24	Square Edge	Aligned	CTAS	0.125	Up
14	64-0632 R 1	4/18/2006	24	Clipped Edge	Aligned	TI	0.01	Up
15	67-0003 R 6	4/19/2006	24	Clipped Edge	Angled	CTI	0.0625	Up
16	64-0612 R 5	4/20/2006	24	Square Edge	Aligned	TI	0.1562	Up
17	66-0194 R 11	4/21/2006	24	Clipped Edge	Aligned	TI	0.125	Up
18	66-0175 R 3	4/21/2006	24	Square Edge	Aligned	CTAS	**	Down
19	66-0171 R 6	4/24/2006	18	Square Edge	Angled	CTI	0.25	Down
20	67-0004 R 5	4/25/2006	18	Square Edge	Aligned	CTI	**	Down
21	66-0153 R 3	4/26/2006	18	Square Edge	Aligned	CTI	**	Down
22	65-0245 R 1	4/27/2006	18	Clipped Edge	Aligned	TI	0.06	Up
23	66-0171 R 2	4/28/2006	24	Square Edge	Angled	CTI	0.25	Up
24	65-0244 R 2	5/1/2006	24	Square Edge	Angled	CTI	0.06	Down
25	66-0199 R 3	5/2/2006	18	Clipped Edge	Aligned	TI	0.03	Up
26	66-0209 R 4	5/3/2006	20	Square Edge	Aligned	TI	0.125	Down
27	65-0275 R 1	5/4/2006	22	Square Edge	Angled	CTI or T	0.06	Down
28	64-0643 R 7	5/4/2006	22	Clipped Edge	Aligned	TI	0.06	Up
29	66-7956 R 3	5/8/2006	24	Square Edge	Angled	CTI	0.06	Down
30	66-0182 R 5	5/9/2006	24	Clipped Edge	Aligned	TI	0.062	Up
31	64-0629 R 8	5/9/2006	24	Square Edge	Angled	CTI	0.0625	Both
32	66-0194 R 14	5/10/2006	20	Square Edge	Aligned	TI	0.063	Down
33	65-0220 R 5	5/10/2006	18	Square Edge	Aligned	TI	**	Down
34	66-0182 R 1	5/11/2006	18	Clipped Edge	Aligned	TI	0.062	Up
35	66-0151 R 1	5/12/2006	20	Square Edge	Aligned	CTI	0.06	Up
36	66-0182 R 6	5/12/2006	24	Clipped Edge	Aligned	TI	0.062	Down
37	66-0194 R 3	5/15/2006	20	Clipped Edge	Aligned	TI	0.125	Up
38	67-0012 R 2	5/15/2006	20	Clipped Edge	Aligned	CTI	0.094	Up
39	66-0164 R 1	5/16/2006	18	Square Edge	Angled	CTI	0.075	Up

Table 1. Original Repairs – Patch Configuration, Crack Length and Orientation (continued)

Test Number	Specimen (Repair) Number	Test Date	Gage Length	Patch Design	Patch Axial Orientation to Riser	Patch OEM	Crack Length	Crack Direction
40	66-0136 R 5	5/16/2006	18	Square Edge	Aligned	TI	**	Up
41	66-7956 R 1	5/16/2006	18	Square Edge	Angled	CTI	0.125	Up
42	64-0628 R 1	5/19/2006	24	Square Edge	Angled	CTI	0.0625	Up
43	64-0628 R 4	5/19/2006	18	Square Edge	Angled	CTI	0.0625	Down
44	66-0158 R 2	5/22/2006	18	Square Edge	Aligned	TI	0.0625	Down
45	65-9408 R 1	5/22/2006	18	Clipped Edge	Aligned	TI	0.0625	Up
46	64-0629 R 5	5/31/2006	18	Square Edge	Angled	CTI	0.0625	Down
47	66-0133 R 1	5/31/2006	18	Square Edge	Aligned	CTI	0.25	Up
48	64-0643 R 3	5/31/2006	24	Clipped Edge	Aligned	TI	0.06	Down
49	67-0001 R 4	6/1/2006	24	Square Edge	Aligned	TI	0.063	Up
50	66-7948 R 1	6/1/2006	24	Square Edge	Aligned	TI	0.06	Down
51	66-0146 R 1	6/5/2006	24	Rounded Corner	Aligned	LM	0.125	Down
52	65-0276 R 1	6/5/2006	20	Clipped Edge	Aligned	TI	0.06	Down
53	66-0198 R 2	6/8/2006	18	Square Edge	Aligned	TI	0.06	Up
54	66-0196 R 6	6/9/2006	20	Square Edge	Angled	CTI	**	Down

** - Can Not Determine Crack Length

2.4.2 New Repair Patch Configuration

All of the specimens in this group were original uncracked wing planks that were extracted from areas of the aircraft close to an original repair for baseline material purposes. These planks were machined into specimens of 18-inch gage length. The weep holes were then precracked to the final crack lengths noted in Table 2. The repairs were based on common repair configurations, with the specific patch design details provided by Warner-Robins AFB from archived data. The patches were bonded with the original surface prep and bonding procedures and materials. The patches were inspected via ultrasonic C-scan after they were cured to ensure there were no voids or delaminations prior to bonding. After the bonding of patches was performed, flash thermography techniques were used to ensure bondline integrity and determine any bondline voids or other issues. All new patched specimens passed NDI inspection. Figure 21 shows a SO surface strain plot of a new repair specimen design.

Table 2. New Repairs - Patch Configuration, Crack Length and Orientation

Test Number	Specimen (Repair) Number	Test Date	Gage Length	Patch Design	Patch Axial Orientation to Riser	Patch OEM	Crack Length	Crack Direction
66	66-0196 R 5 P	6/28/2006	18	Square Edge	Aligned	AFRL/MLSA	0.257	Up
67	66-7955 R 2 P	6/29/2006	18	Square Edge	Aligned	AFRL/MLSA	0.250	Up
68	64-0612 R 1 P	6/28/2006	18	Square Edge	Aligned	AFRL/MLSA	0.250	Up
69	64-0628 R 1 P	6/29/2006	18	Square Edge	Aligned	AFRL/MLSA	0.785	Up

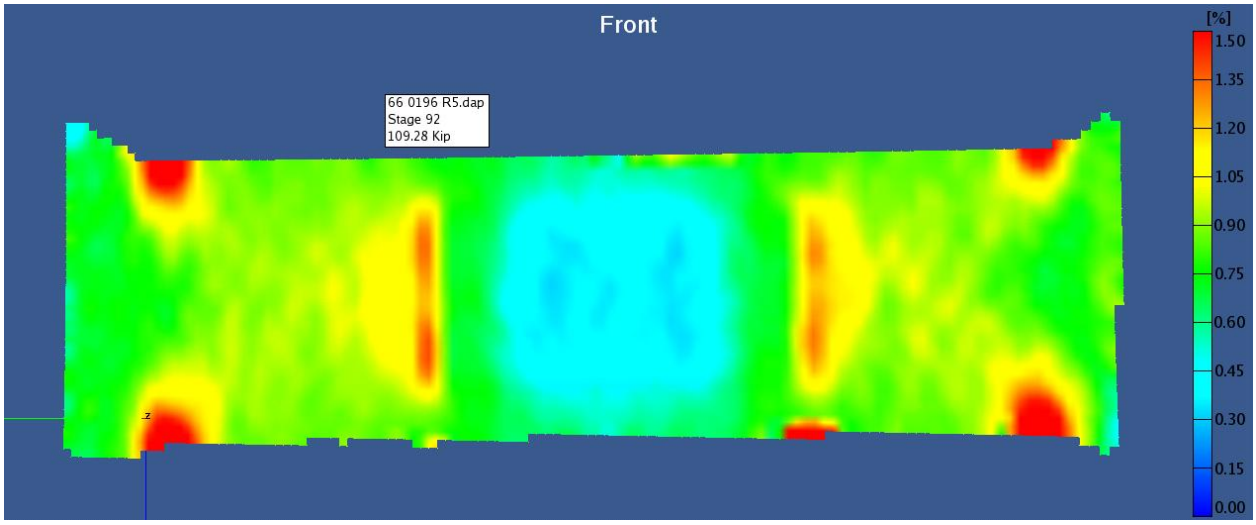

Figure 21. New Bonded Patch Design - Aligned Square Edge Patch.

2.4.3 Unrepaired Residual Strength Tests

It was desired to test a small number of specimens with unrepaired cracked weep holes to provide a baseline residual strength. This would serve two purposes; the first of which is to provide a basis for strength knockdown comparison in the event that a repaired specimen failed through the repaired weep hole, and secondly to provide a strength knockdown for a worst case scenario in which a cracked weep hole was missed during inspection and never repaired. The specimens were fabricated from pristine (uncracked) panels that were cut from aircraft areas just adjacent to a repair. The specimens were EDM notched and precracked to nominal target crack lengths to provide a rudimentary measure of residual strength with a sharp crack originating at the weep hole. Table 3 details the unrepaired residual strength specimens that have been cracked. The precracking procedure is covered in detail in Section 2.4.5.

Table 3. Residual Strength – Crack Length and Orientation

Test Number	Specimen (Repair) Number	Test Date	Gage Length	Target Crack Length	Actual Crack Length	Crack Direction
57	65-0244 R 2 P	6/23/2006	18	0.250	0.254	Up
58	67-UNKN R 6 P	6/23/2006	18	0.500	0.511	Up
59	65-0276 R 1 A P	6/26/2006	18	0.250	0.256	Up
60	66-0153 R 1 P	6/26/2006	18	0.250	0.252	Up
61	67-0029 R 6 P	6/27/2006	18	0.125	**	**
62	65-0276 R 1 B P	6/27/2006	18	0.375	0.375	Up
63	66-UNKN R 8 P	6/27/2006	18	0.500	0.504	Up
64	66-0151 R 1 P	6/28/2006	18	0.125	**	**
65	66-0136 R 5 P	6/28/2006	18	0.375	0.402	Up

** - specimen broke during precracking

In addition, it was desired to test original cracks to determine if there was any difference between the unpatched residual strength tests and original cracked panels. Any difference could be attributed to the precracking method, as time constraints would not allow the original flight load spectrum and loading conditions to generate cracks similar to the original. To provide a basis for comparison, two original planks were selected for testing due to their long cracks and "up crack" orientation. These specimens were stripped of the original patches and tested in the same manner as the unrepaired residual strength tests. These specimens are detailed in Table 4. The procedure used to strip the original patches is outlined in Section 2.4.4.

Table 4. Residual Strength – Original Cracks with Stripped Patches

Test Number	Specimen (Repair) Number	Test Date	Gage Length	Recorded NDI Crack Length	Crack Direction
55	66-0148 R 2	6/13/2006	18	0.375	Up
56	67-0021 R 6	6/14/2006	18	0.250	Up

2.4.4 Patch Stripping Procedure

In addition to the unpatched residual strength specimens, it was desirable to test a small number of original repairs for residual strength with the patches removed. This was intended to quantify any difference in residual strength, as well as determine if the original patch had arrested the crack. To this end, two candidate planks with relatively long cracks were selected from the population of repairs. Specimen numbers 66-0148R2 and 67-0021R6 were selected as they were original repairs with crack lengths measured to be 0.375 and 0.250 inches, respectively.

The specimens were prepped for patch stripping by using a rotary air tool with a 3M radial bristle disk. The bristle disk removed all excess sealant and paint from around the patch area without inducing damage. The patches were stripped by heating the material surrounding the patch edge, along with any exposed aluminum on the backside of the patch. Care was exercised to not overheat the substrate material. The adhesive became soft after the base material was hot enough, then the patch could be carefully pried away from the surface using a sharp putty knife to peel through the adhesive. After stripping, the skin material was checked via conductivity measurements to ensure the temper was not adversely affected. The conductivity of the entire specimen was compared, all readings were within the expected range for the parent material, and no changes in conductivity were noted across the entire specimen.

2.4.5 Precracking Procedure

The specimens to be patched with new patches, as well as those to be tested for residual strength with no repair, required sharp cracks of various lengths. In all cases, the sharp cracks were to be "up cracks" originating at the upper edge of the weep hole and growing up the riser, with the crack width spanning the entire riser thickness. To facilitate the precracking required to grow the sharp cracks, wire EDM (Electrical Discharge Machining) starter notches were cut from the weep hole vertically into the riser. The wire EDM notches were cut through the riser thickness with the minimum diameter wire available to produce the sharpest starter notch tip. The EDM wire used was 0.015-inch in diameter, creating a notch width of approximately 0.017 inches and a tip radius of 0.009 inches. The EDM starter notch lengths were held to 0.050 inches shorter than the final desired crack length to ensure the sharp crack tip was long enough per ASTM E399[4] guideline for minimum valid precrack crack length.

Once the EDM starter notch was completed, the specimen was loaded in cyclic flexure using a three point bending fixture. An axial strain gage was adhered to the top surface of the riser to ensure the cyclic peak stress did not exceed 50 ksi for the 0.25-inch crack length specimens. Longer crack length specimens did not require as much load, so peak cyclic stresses were limited to 40 and 30 ksi for the 0.375- and 0.50-inch cracks, respectively. The centroid of the specimen section runs through the center of the riser, just above the skin. This location roughly coincides with the bottom edge of the weep hole. Flexure loading in this structure has peak tensile stresses at the upper outer fiber of the riser, peak compressive stresses in the lower outer fiber of the skin, and zero axial stress at the neutral axis (effectively the centroid). Due to the section properties and the loading profile, the root of the riser was effectively shielded from load, thus requiring larger than normal loads required to initiate and grow a crack up the riser. As the crack length increased, this load shielding effect was reduced, and lower loads could be used to initiate and grow cracks. As noted in Table 9, both of the shortest crack length (0.125 inch final length) specimens were accidentally destroyed due to the load shielding effect while attempting to initiate and grow the precrack.

[4] "Standard Test Method for Plane-Strain Fracture Toughness of Metallic Materials", ASTM E 399, American Society for Testing and Materials, revised 2001.

2.5 TEST PROCEDURE

2.5.1 Handling and Machining of Rough Cut Planks

The rough cut planks were shipped from Warner Robins AFB to the AFRL via FedEx Commercial Freight. Upon receipt of the planks, the shipment was documented and inspected to ensure a complete shipment and track progress of the test effort. The planks were then sorted according to repair type and suitability of the individual rough cut planks. Planks with undesirable features or insufficient overall length were set aside for later disposition. The desirable candidate specimens were then sorted into a conventional specimen group and a riser 4 repair group. This was done to expedite the machining of specimens, as riser 4 repair specimens required specific operations beyond the typical specimen machining operations. The specimens were laid out using the most appropriate specimen design for each particular plank and repair configuration. Upon layout, the planks were marked with standardized specifications detailing the specimen type to be machined, the repair number, and any specific instructions that pertained to the plank or specimen machining. The specimens were then machined in groups to minimize down time associated with tooling changes required for specific machining operations. The specimens were generally machined in groups of 4 to 7 planks per group.

2.5.2 Specimen Preparation for Test

After machining, the specimens were delivered to the AFRL/MLSC mechanical testing laboratory for test preparation. The specimens were inspected for machining defects and wiped down with a rag if necessary. The sealant was removed from the strain gage locations on the riser patch with 3M rotary bristle disks. The specimen was wiped down again and the strain gages were bonded in the appropriate locations. An individual data sheet was prepared for each specimen, and measurements for the specific cross sections were taken and recorded. The specimen was inspected with an optical magnifying glass in an attempt to detect any cracks at the unrepaired weep holes. All cross section locations (see Section 2.6.1 for further detail) were marked on the strain gaged riser bay. The opposite riser bay, and outside (OML patch side) surfaces were cleaned with acetone across the entire gage section and into the blend radii. The areas to be speckle painted were masked off and a matte white basecoat of paint was applied. After sufficient drying time, the black paint speckles were applied with a specially modified nozzle to spray larger than normal droplets of paint. The specimen was speckle painted in this manner to provide an optimum speckle density for the standoff distance used in this program.

2.5.3 Test Procedure

The procedure for the residual strength test began with the mounting of the specimen in the grips. Each of the 0.375-inch diameter fasteners in the grip area of the specimen was torqued to 45 ft-lbs, and the 0.50-inch diameter fasteners in the same area were torqued to 80 ft-lbs. The strain gages were wired into the data acquisition computer interface and checked for correct function. Pre-test digital pictures were taken of the specimen from multiple angles for documentation purposes. The data acquisition computer, as well as the computer running the SO acquisition was set up and proper signals were verified. The alignment checks were run (described in Section 2.3.3) and any alignment adjustments were made, if needed. The alignment data also provided a function check of the data and SO acquisition units. The specimen was brought to nominal zero load, all gage channels were zeroed, and the acquisition units were started a few seconds prior to the test. Upon confirmation that images and data were being acquired, the 458.91 MicroProfiler was started to begin the test. As the specimen loaded, the live strain data was checked for proper behavior. Upon specimen failure, the acquisition computers were stopped and the MicroProfiler was stopped. The maximum displayed load was recorded from the 458 controller and the cross section through which the failure occurred was also recorded on the specimen data sheet. Final pictures of the specimen and failure section were taken with a handheld digital camera, after which the specimen was unbolted from the grip assembly.

2.5.4 Post-Test Procedures

Directly following each residual strength test, the specimen was unbolted from the test fixtures and examined for any unusual test artifacts. The failure zone, as well as the patches and surrounding material, were closely examined. The SO data was post processed to provide typical plots and strain maps, and once that data was generated, the SO results were closely inspected for any patch failures or unexpected behavior. All further strain gage and mechanical data was reduced and summary sheets were updated.

2.6 TEST DATA REDUCTION

2.6.1 Test Specimen Cross Section Data

All specimen section dimensions were recorded on individual data sheets. The sections were named alphabetically from A to H, although not all named sections were necessarily present in each specimen. Generally, each specimen could be oriented with the axial centerline facing either direction (outboard facing up or inboard facing up) for test purposes. However,

each specimen section was named in the same manner, from outboard to inboard. Figure 22 is provided as a general layout to aid the section descriptions and typical locations, as follows. Section A was the furthest outboard, located approximately 1-inch inside of the blend radius tangent point. Section B was located as close to the outboard edge of the riser patch as possible, but actual location was dictated by the patch sealant. Section C and D correspond to the strain gage locations on the riser patch, located at 1/3 and 2/3 of the patch length, respectively. Sections E1 and E2 were the cross sections through the rib clip holes, also coinciding with the inboard most edge of the riser patch sealant. Occasionally E1 and E2 were drilled through an extended riser patch. This was noted on the data sheet if that was the case. Section F was located midway between E and Gw, or midway between E and H if no weep hole was present. Section Gw was the cross section through the unrepaired weep hole (not present in the gage length on all specimens). Section H was the furthest inboard section, located approximately 1 inch outboard of the tangent point of the blend radius. All section locations were marked on each specimen in marker, and the specific gage length locations of each were noted on the data sheet with the corresponding cross section dimensions. Additional sections were named and noted on the individual data sheet if an abnormal sectional feature was present. These sections were well documented on an individual basis should failure occur due to the abnormality.

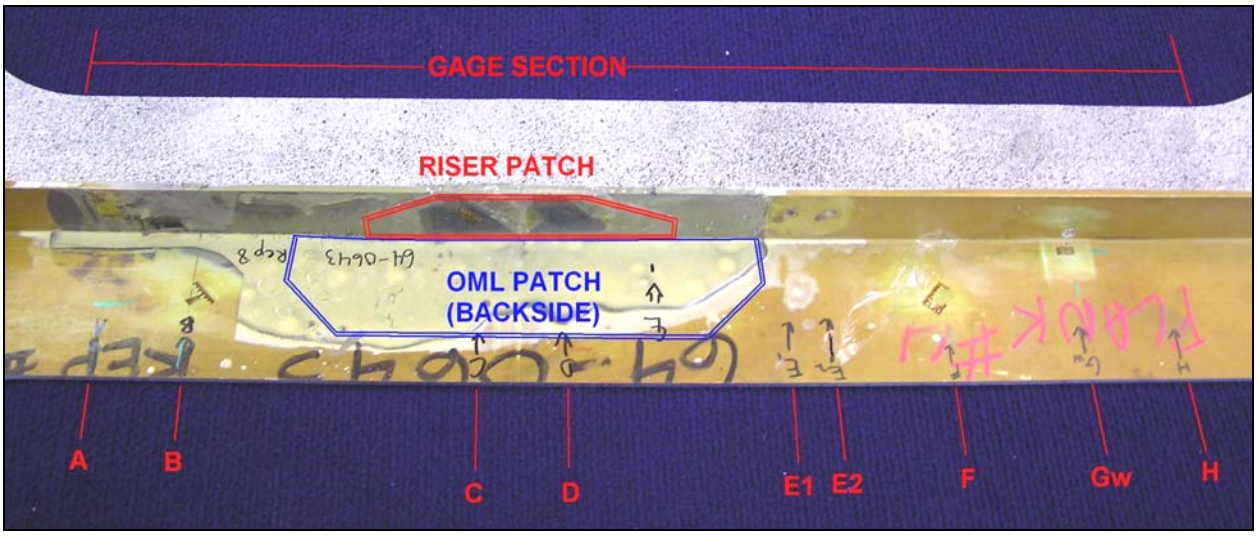

Figure 22. Typical Layout of Gage Length Cross Sections and Locations.

2.6.2 Data Reduction

All stated load, strain, and actuator displacement data referenced or tabulated is the reduced data as recorded with the National Instruments modular data acquisition system, acquiring signals at 5 Hz. The data were reduced with a template spreadsheet using max/min functions as well as plotting features to ensure the data were valid.

2.6.3 Data Calculations

All “nominal” stress calculations were based on the maximum load data mentioned in Section 2.6.2. The area used for stress calculations was the average values for the minimum gross cross sectional area for each specimen. All “failure zone” stress calculations were made using the same maximum load value, but using the actual cross sectional area through which the failure initiated, including area losses for holes or other atypical gage section features. In cases where the failure zone stress is denoted with a double asterisk in Table 5, the failure section ran through multiple cross sections or through a region where the area could not be calculated. This generally occurred due to the presence of sealant interfering with a section measurement, a failure section that deviated from a perpendicular plane, or a failure occurring in the blend radius or grip region where cross section measurements were not taken.

It should be noted that the patch dimensions, thicknesses, stiffness, or other properties were not used in any calculations. No estimates or measurements of patch stiffness, modulus, or other quantification of load or strain response through the patch were made.

SECTION 3
RESULTS

3.1 RESULTS OF ORIGINAL REPAIRS

The residual strength results of the original repairs are detailed in Table 5. The table lists the failure loads, stresses, and failure section (location) details, along with specific comments for many specimens. Specimen comments denoted in red indicate an invalid specimen, due to such artifacts as a saw cut in the riser or a CTAS repair. The CTAS repairs were disqualified from the data set because the repairs had less than 10 years of accumulated flight time. Asterisks (**) in the data set indicate a failure section area that could not be calculated, typically due to the presence of patch or sealant material preventing the accurate measurement of the cross section, or other reasons.

The loads and stresses listed for each specimen in the table are the maximum load recorded prior to specimen failure. The stresses listed are calculated with the maximum load over the listed area, being the gross stress locations in the gage section of the specimen, or the failure stress at the cross section of the failure. This is covered in more detail in Section 4.6.3.

The average residual strength (excluding the invalid specimens mentioned previously) of all specimens with no unrepaired weep holes in the gage section is 83.2 ksi based on nominal section stress. The average residual strength of specimens that did have unrepaired weep holes in the gage section was 81.6 ksi.

Table 5. Summary of Original Repair Residual Strength Data

Test Number	Specimen (Repair) Number	Test Date	Gage Length	Max Load (lbf)	Max Nominal Stress (psi)	Max Failure Section Stress (psi)	Failure Location	Patch Failure?	Comments
1	66-0156 R 1	11/21/2005	24	109118	79706	82341	Unrepaired weephole, Gage Section	No	
2	66-0209 R 8	3/3/2006	24	108337	81267	83038	Unrepaired weephole, Gage Section	No	
3	64-0643 R 9	3/8/2006	24	107825	82288	**	Unrepaired weephole, Grip Section	No	Grip related failure
4	64-0643 R 8	3/17/2006	24	101031	78621	**	Unrepaired weephole, Grip Section	No	Grip related failure
5	66-0199 R 1	3/20/2006	24	109783	81137	78107	Unrepaired weephole, Gage Section	No	Reinforced skin thickness at unrepaired weephole
6	66-7955 R 2	3/23/2006	24	107940	77983	81496	Unrepaired weephole, Gage Section	No	
7	65-0245 R 2	3/24/2006	24	113586	83103	**	Rib Clip Hole, down riser, under OML Patch	Yes, OML	OML patch flew off after specimen broke - EPS
8	66-0168 R 1	4/6/2006	24	112878	86271	**	Failure in Grip Section	Yes, OML	No holes in gage section - Engine Pylon Specimen
9	66-0209 R 9	4/10/2006	24	84899	64638	**	Riser saw cut	No	Deep saw cut in riser - Invalid Specimen
10	64-0643 R 5	4/11/2006	24	89630	65698	**	Riser saw cut	No	Deep saw cut in riser - Invalid Specimen
11	64-0612 R 2	4/12/2006	24	107129	77551	79880	Unrepaired weephole, Gage Section	No	
12	66-0153 R 1	4/13/2006	24	110114	81901	83963	Unrepaired weephole, Gage Section	No	
13	67-0016 R 5	4/13/2006	24	104211	77132	81400	Unrepaired weephole, Gage Section	No	CTAS Repair - Invalid Specimen
14	64-0632 R 1	4/18/2006	24	113825	83419	85604	Rib Clip Hole	No	
15	67-0003 R 6	4/19/2006	24	114453	79896	**	Unrepaired weephole, Blend Radius	Yes, OML	No holes in gage section - Engine Pylon Specimen
16	64-0612 R 5	4/20/2006	24	112536	82817	84855	Rib Clip Hole	No	
17	66-0194 R 11	4/21/2006	24	106628	84107	79181	Unrepaired weephole, Gage Section	No	Reinforced skin thickness at unrepaired weephole
18	66-0175 R 3	4/21/2006	24	107788	81870	83870	Unrepaired weephole, Gage Section	No	CTAS Repair - Invalid Specimen
19	66-0171 R 6	4/24/2006	18	112249	79949	81651	Rib Clip Hole	No	No unrepaired weepholes in gage section
20	67-0004 R 5	4/25/2006	18	109600	78522	80187	Rib Clip Hole	No	No unrepaired weepholes in gage section
21	66-0153 R 3	4/26/2006	18	118188	81024	**	Rib Clip Hole thru elongated Riser Patch	No	Thick skin
22	65-0245 R 1	4/27/2006	18	133865	84860	83777	Unrepaired weephole, Gage Section	No	Thick skin, no unrep weepholes
23	66-0171 R 2	4/28/2006	24	110955	78929	80537	Unrepaired weephole, Gage Section	No	3 weepholes in gage section
24	65-0244 R 2	5/1/2006	24	116168	83628	85556	Rib Clip Hole	No	No unrepaired weepholes in gage section
25	66-0199 R 3	5/2/2006	18	110992	84433	**	Rib Clip Hole thru elongated Riser Patch	No	No unrepaired weepholes in gage section
26	66-0209 R 4	5/3/2006	20	109906	83004	85251	Rib Clip Hole	No	No unrepaired weepholes in gage section
27	65-0275 R 1	5/4/2006	22	109296	81098	**	Rib Clip Hole thru elongated Riser Patch	No	
28	64-0643 R 7	5/4/2006	22	113757	76969	85400	Unrepaired weephole, Gage Section	No	
29	66-7956 R 3	5/8/2006	24	107916	78171	82247	Unrepaired weephole, Gage Section	No	
30	66-0182 R 5	5/9/2006	24	110577	81734	82613	Rib Clip Hole	No	
31	64-0629 R 8	5/9/2006	24	110938	81121	**	Rib Clip Hole, down riser, under OML Patch	No	OML patch flew off after specimen broke
32	66-0194 R 14	5/10/2006	20	113159	81079	82489	Unrepaired weephole, Gage Section	No	

Table 5. Summary of Original Repair Residual Strength Data (Continued)

Test Number	Specimen (Repair) Number	Test Date	Gage Length	Max Load (lbf)	Max Nominal Stress (psi)	Max Failure Section Stress (psi)	Failure Location	Patch Failure?	Comments
33	65-0220 R 5	5/10/2006	18	112579	83189	**	Rib Clip Hole	No	No unrepaired weepholes in gage section
34	66-0182 R 1	5/11/2006	18	108923	86124	85259	Rib Clip Hole	No	No unrepaired weepholes in gage section
35	66-0151 R 1	5/12/2006	20	108771	85407	79949	Unrepaired weephole, Gage Section	No	Reinforced skin thickness at unrepaired weephole
36	66-0182 R 6	5/12/2006	24	110000	82781	85521	Rib Clip Hole	Yes, OML	OML patch flew off after specimen broke
37	66-0194 R 3	5/15/2006	20	115039	86616	**	Rib Clip Hole thru elongated Riser Patch	No	No unrepaired weepholes in gage section
38	67-0012 R 2	5/15/2006	20	111371	83455	85103	Unrepaired weephole, Gage Section	No	
39	66-0164 R 1	5/16/2006	18	112134	84520	87409	Rib Clip Hole	No	No unrepaired weepholes in gage section
40	66-0136 R 5	5/16/2006	18	106036	86823	89000	Rib Clip Hole	No	No weepholes in gage section, thin skin specimen
41	66-7956 R 1	5/16/2006	18	106805	84200	83662	Unrepaired weephole, Gage Section	No	
42	64-0628 R 1	5/19/2006	24	114331	85431	86545	Rib Clip Hole	No	No holes in gage section - Engine Pylon Specimen
43	64-0628 R 4	5/19/2006	18	108361	79906	82099	Rib Clip Hole	No	No unrepaired weepholes in gage section
44	66-0158 R 2	5/22/2006	18	110754	84195	85959	Rib Clip Hole	Yes, OML	OML patch flew off after specimen broke
45	65-9408 R 1	5/22/2006	18	113178	87559	86871	Rib Clip Hole	No	No unrepaired weepholes in gage section
46	64-0629 R 5	5/31/2006	18	112360	84738	83355	Rib Clip Hole	No	No unrepaired weepholes in gage section
47	66-0133 R 1	5/31/2006	18	105475	77520	**	Failure in Grip Section, Riser 4	No	Grip related failure
48	64-0643 R 3	5/31/2006	24	102648	76538	**	Failure in Grip Section, Riser 4	No	Grip related failure
49	67-0001 R 4	6/1/2006	24	108624	83361	78006	Unrepaired weephole, Gage Section	No	Large reamed unrepaired weephole
50	66-7948 R 1	6/1/2006	24	110858	78982	83107	Unrepaired weephole, Gage Section	No	
51	66-0146 R 1	6/5/2006	24	116632	87153	**	Failure in Grip Section, Riser 4	Yes, OML	Grip related failure
52	65-0276 R 1	6/5/2006	20	113196	84539	84898	Rib Clip Hole	Yes, OML	Square edge riser patch w/ clipped edge OML
53	66-0198 R 2	6/8/2006	18	110089	85012	**	Rib Clip Hole	No	No unrepaired weepholes in gage section
54	66-0196 R 6	6/9/2006	20	102344	75090	76700	Rib Clip Hole	No	No unrepaired weepholes in gage section

** - Failure Section Varies

The majority of the original repairs sustained no patch related failures. These specimens generally failed in the gage (reduced) section of the aluminum away from the patch. For these typical cases, the SO results were checked to confirm there were no delaminations or other patch events, and then saved for future use. For brevity, only a representative SO response is presented in this report, rather than listing each individual specimen. Figure 23 displays a typical SO response for an original repair, with the strain scale changed from high to low scale to better illustrate the surface strain through the specimen and the OML patch. In this case, the original repair was a square edge patch design.

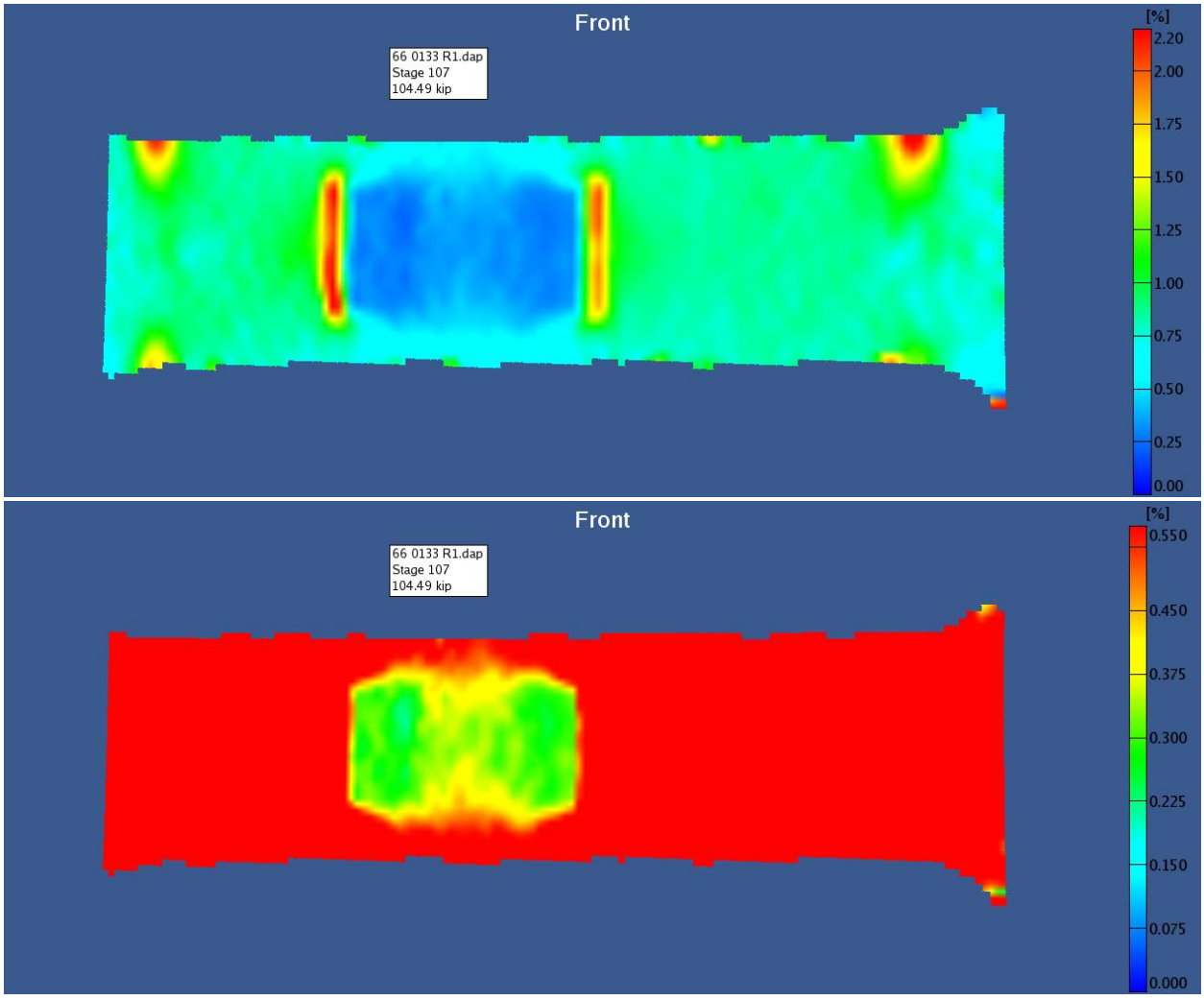

Figure 23. Typical SO Response of Original Repairs (top = high scale, bottom = low scale).

Of the 54 tests performed, only 9 specimens experienced a patch related failure. A summary of the patch failure events is provided in Table 6. The table lists the type of failure sustained as well as the load and stress at which the failure occurred. In all cases, the specimen continued to load up beyond the event load, so the ultimate strength data is also provided for each specimen. A more detailed description of each failure, including SO results, follows below in the order it is listed in Table 6.

Table 6. Summary of Original Repairs with Patch Failure Events

			Specimen Failure			Patch Failure		
Test Number	Specimen (Repair) Number	Test Date	Max Load (lbf)	Max Nominal Stress (psi)	Specimen Failure Location	OML Patch Failure Event Type	Event Load (lbs)	Event Stress (ksi) Far Field
7	65-0245 R 2	3/24/2006	113586	83103	Rib Clip Hole	Delam then Disbond	105470	77.17
8	66-0168 R 1	4/6/2006	112878	86271	Grip & Blend Radius	Delamination	110550	84.49
15	67-0003 R 6	4/19/2006	114453	79896	Blend Radius	Delamination	108300	75.60
31	64-0629 R 8	5/9/2006	110938	81121	Rib Clip Hole	Delam then Disbond	99610	72.84
36	66-0182 R 6	5/12/2006	110000	82781	Rib Clip Hole	Delam then Disbond	110440	75.59
38	67-0012 R 2	5/15/2006	111371	83455	Unrep Weep Hole	Delamination	70000	52.45
44	66-0158 R 2	5/22/2006	110754	84195	Rib Clip Hole	Disbond	65704	49.95
51	66-0146 R 1	6/5/2006	116632	87153	Grip & Blend Radius	Delamination	98500	73.00
52	65-0276 R 1	6/5/2006	113196	84539	Rib Clip Hole	Delamination	104000	77.60

Specimen number 65-0245 R 2 had a patch with a clipped edge, aligned OML patch (TI repair) that began to delaminate at the corner of the patch at approximately 77 ksi. The delamination/disbond grew under increasing load across the edge of the specimen, then increasing in size under the skin with increasing load. The specimen failed at 83.1 ksi. Figure 24 shows the strain field of the patch failure at the first detectable occurrence as well as the final maximum extent of the delamination, just prior to sample failure. Note that the scale used in the figure has been reduced to more clearly show the patch failure. The OML patch became completely disbonded upon failure and separated from the specimen.

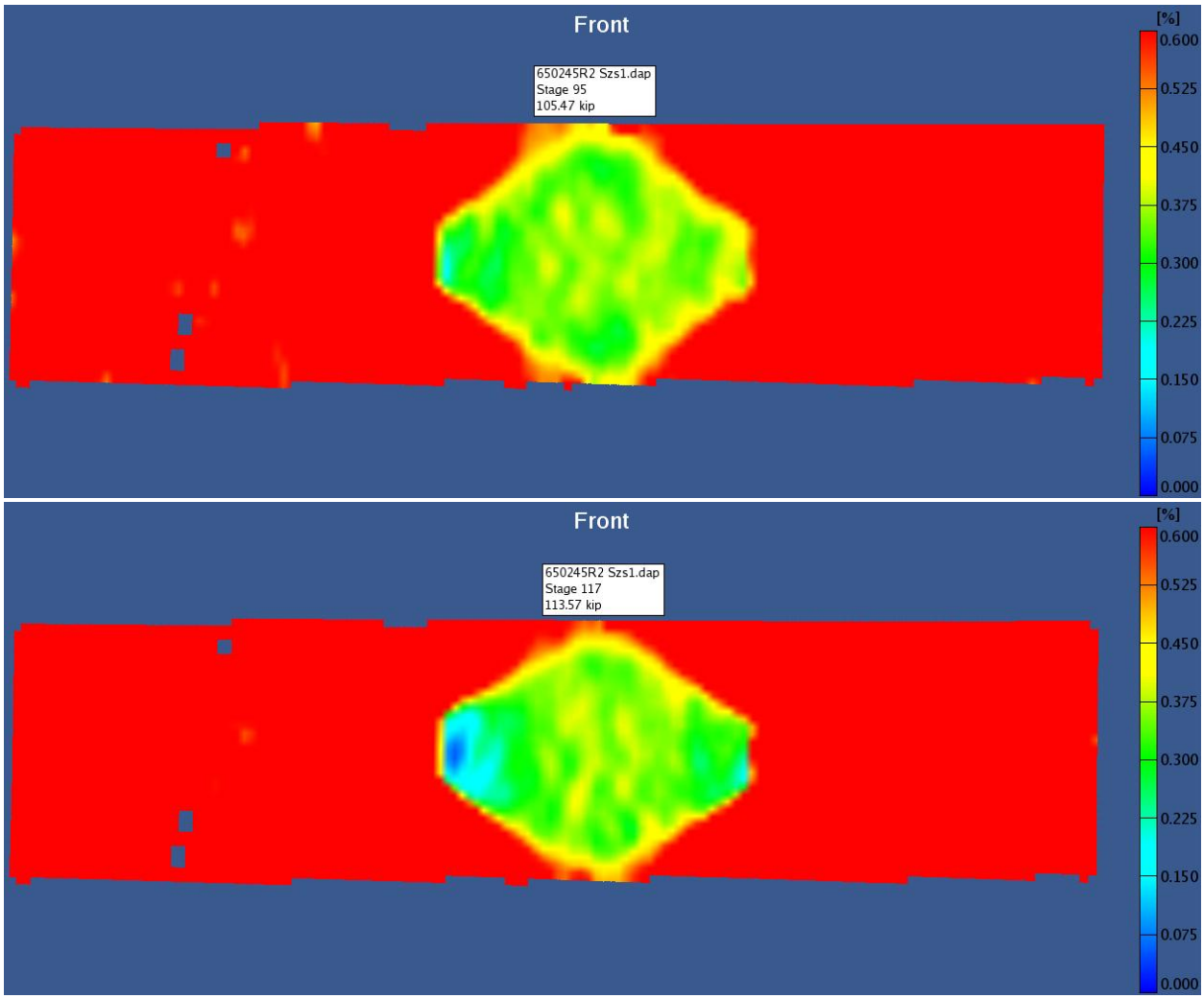

Figure 24. OML Patch Delamination; Repair 65-0245 R 2.

Specimen number 66-0168 R 1 had a clipped edge, aligned OML patch (TI repair) that began to delaminate at the corners of the patch at approximately 84 ksi. The delaminations grew under increasing load across the edge of the specimen, eventually joining into a single delamination and growing under the skin with increasing load. The specimen failed at 86.3 ksi. Figure 25 shows the strain field of the patch failure at first detectable occurrence as well as the final maximum extent of the delamination, just prior to substrate failure.

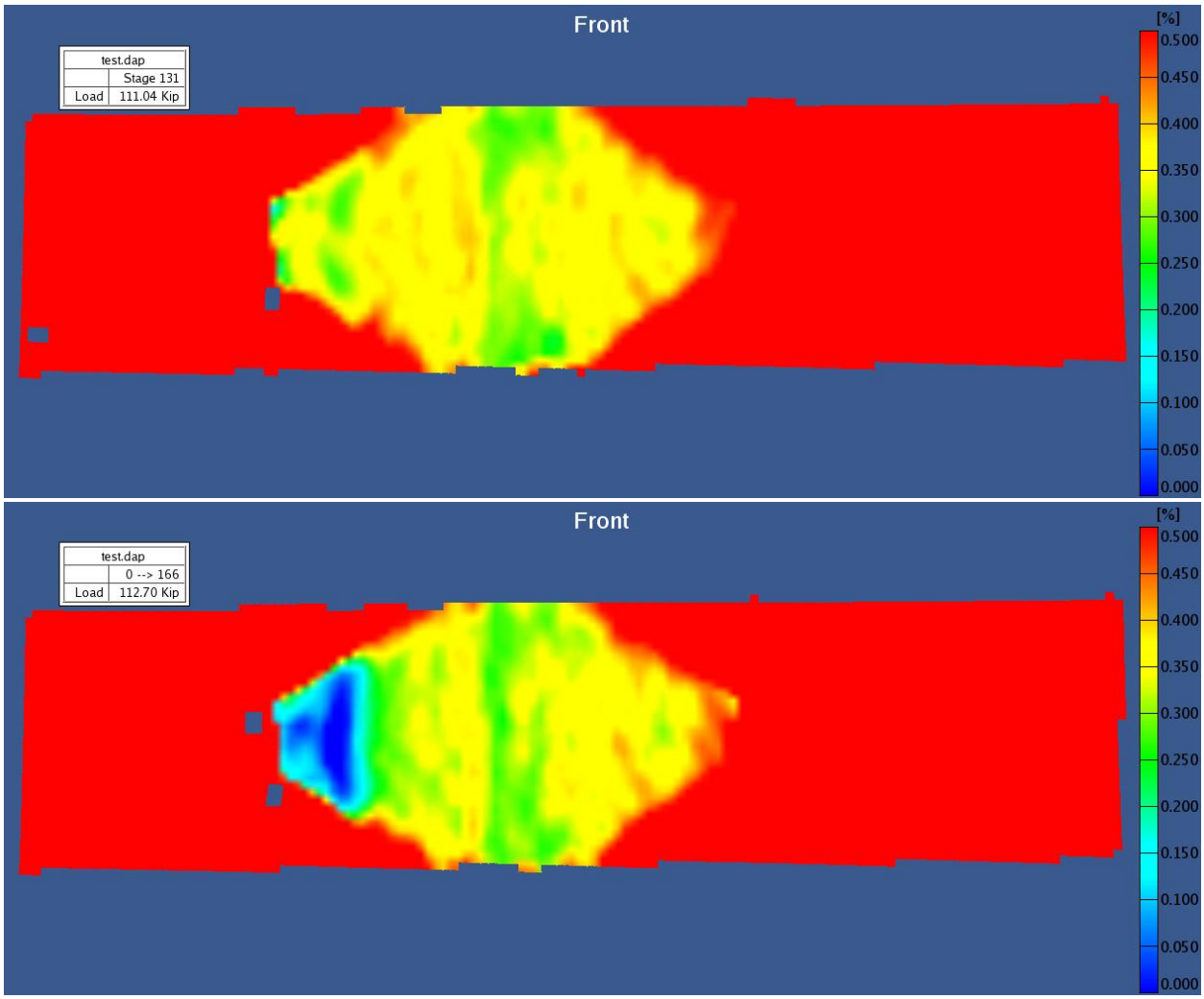

Figure 25. OML Patch Delamination; Repair 66-0168 R 1.

Repair number 67-0003 R 6 had a clipped edge, angled OML patch (CTI repair) that began to delaminate at central tip of the patch at approximately 75 ksi. The delamination grew slightly under the patch with increasing load. The specimen failed at 79.9 ksi. Figure 26 shows the strain field of the patch failure at first detectable occurrence as well as the final maximum extent of the delamination, just prior to substrate failure.

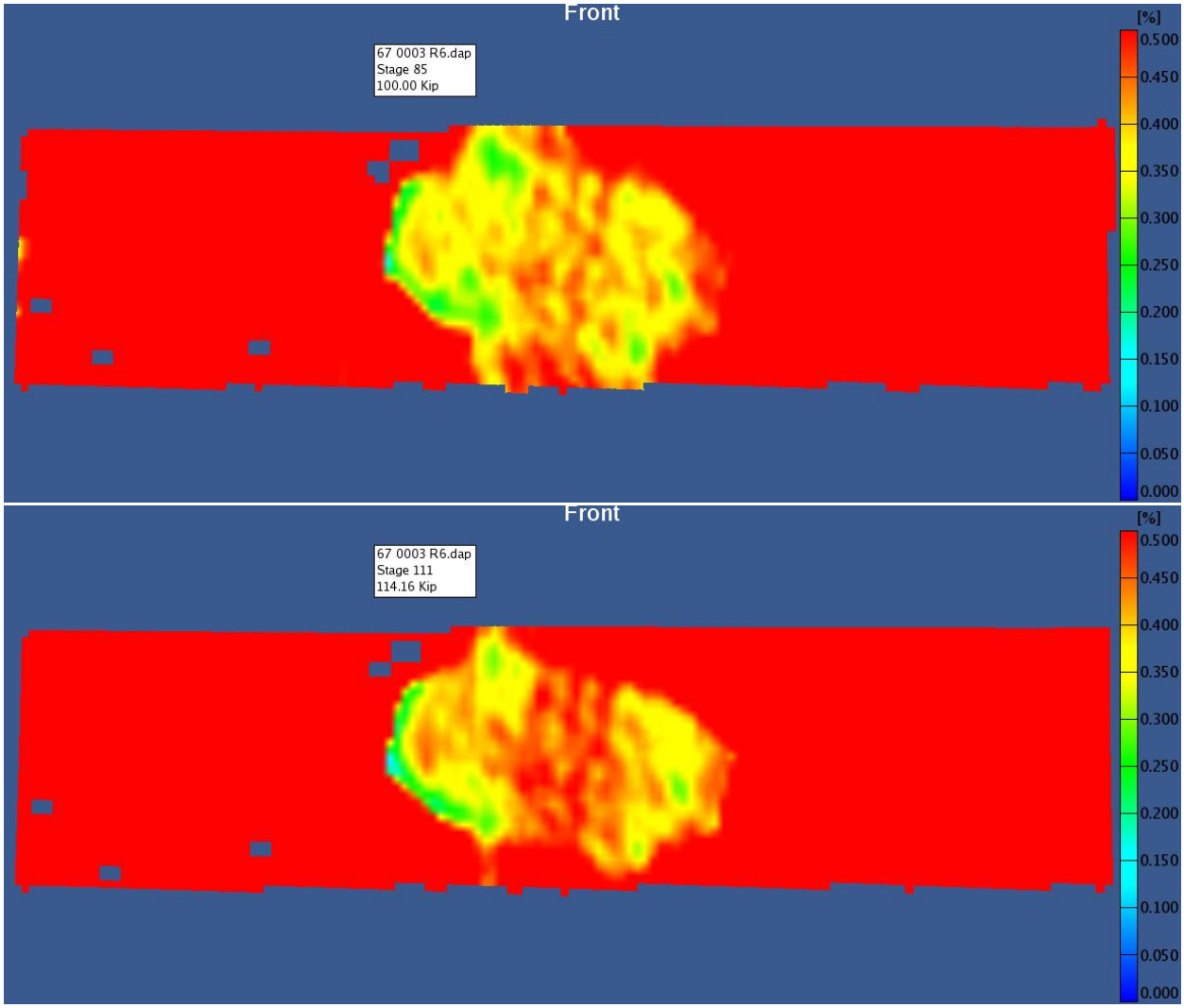

Figure 26. OML Patch Delamination; Repair 67-0003 R 6.

Repair number 64-0629 R 8 had a square edge, angled OML patch (CTI repair) that began to delaminate at central tip of the patch at approximately 73 ksi. The delamination grew extensively under the patch with increasing load. The specimen failed at 81.1 ksi. Figure 27 shows the strain field of the patch failure at first detectable occurrence as well as the final maximum extent of the delamination, just prior to substrate failure.

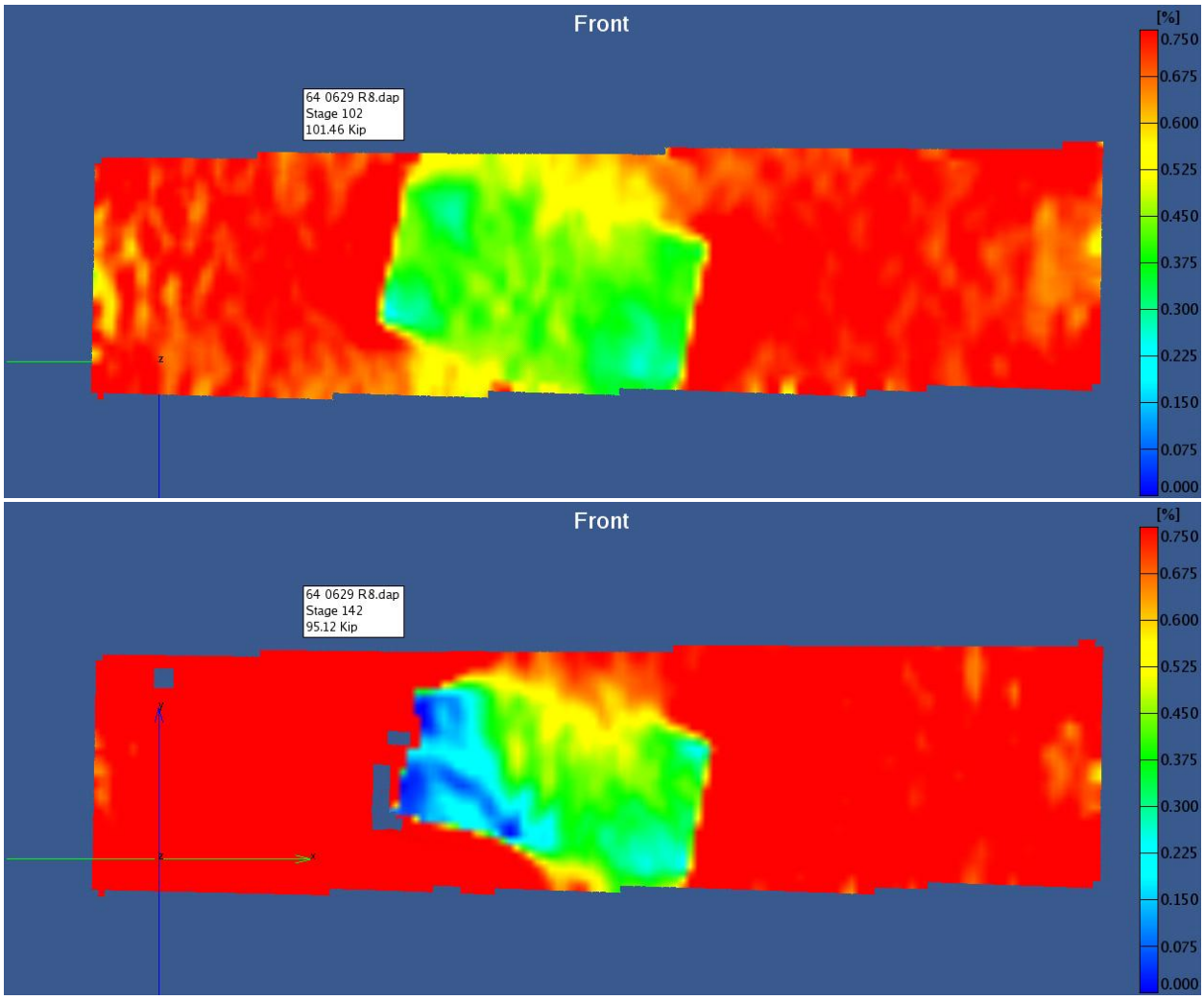

Figure 27. OML Patch Delamination; Repair 64-0629 R 8.

Repair number 66-0182 R 6 had a clipped edge, aligned OML patch (TI repair) that appeared to become disbonded from the substrate at approximately 75.6 ksi. The load dropped simultaneously with the disbond event, indicating that the load carried by the patch was released. The load dropped approximately 5,000 lbs (to a stress of 71.6 ksi). The specimen continued loading from that point to the ultimate stress of 82.8 ksi. Figure 28 shows a progression of SO results displaying the patch strain field just to the disbond event, after the disbond event, and at the ultimate load of the specimen. Note the patch is "cold" after the disbond event, indicating little to no strain being carried through the patch. The area to the right of the patch appears to be at high strain, but this is actually a large crack in the sealant that the SO system incorrectly interpreted as high strain (speckles moved far apart). The OML patch became completely disbonded upon substrate failure and separated from the specimen.

The specific failure mode of this specimen is discussed in more detail in an AFRL/MLSA composite failure analysis report entitled *"C-141 Weep Hole Boron Patch Characterization" (Ref #AFRL/MLS 06-091).*

Repair number 67-0012 R 2 had a clipped edge, angled OML patch (CTI repair) that delaminated or disbonded at the lower edge of the patch at approximately 52 ksi. The delamination grew slightly under the patch with increasing load. However, the SO surface strain data surrounding the patch indicated that the patch continued to attract and carry load after the delamination event, indicating that the delamination was in the outermost plies and only affected surface strain. The specimen failed at 83.5 ksi. Figure 29 shows the strain field of the patch just prior to the failure (top), just after the failure at first detectable occurrence (middle), as well as the final maximum extent of the delamination (bottom) just prior to substrate failure. Note that the scale used in the figure has been reduced to more clearly show the patch failure. The specific failure mode of this specimen is further described in reference #AFRL/MLS 06-091.

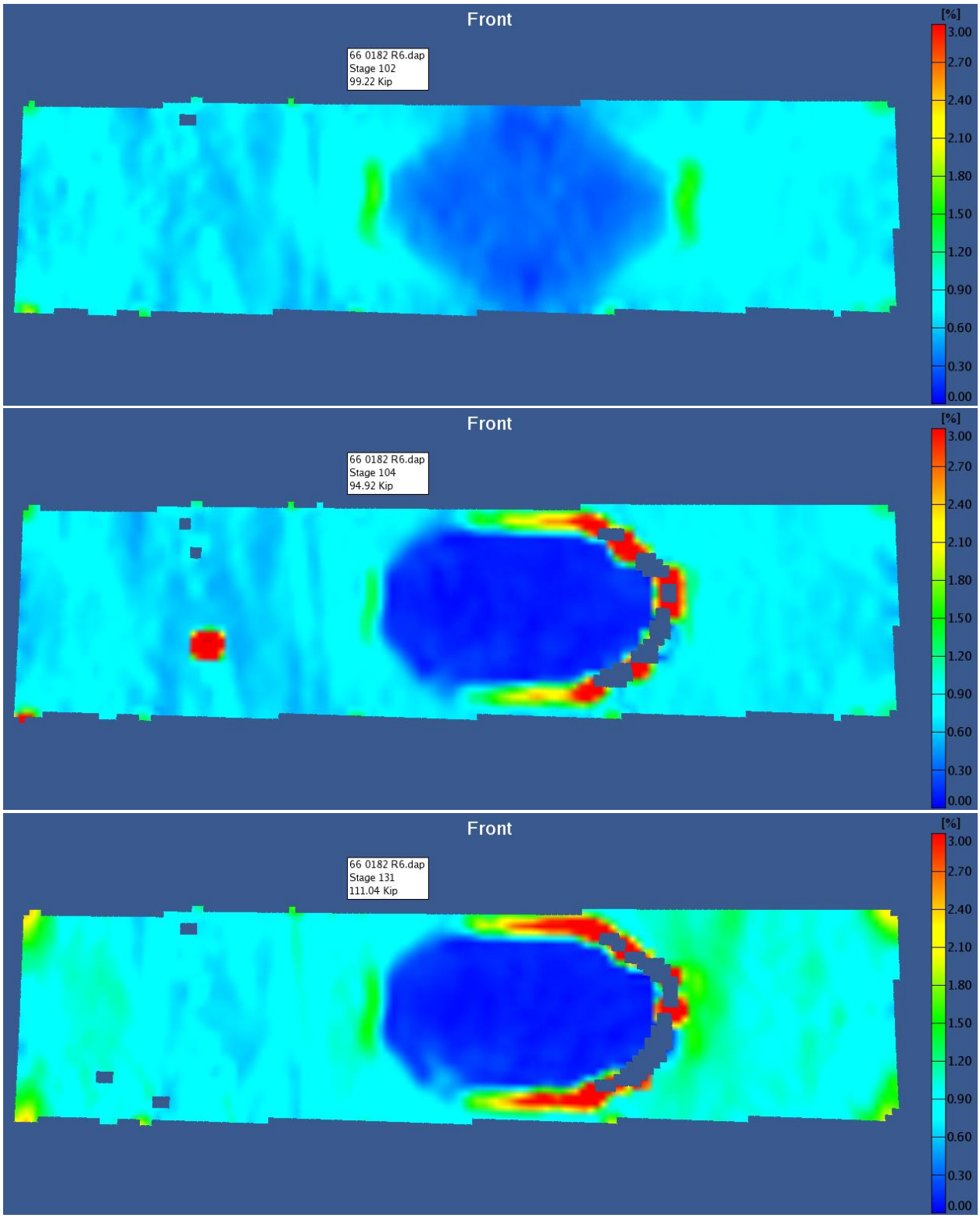

Figure 28. OML Patch Failure Disbond: Repair 66-0182 R 6.

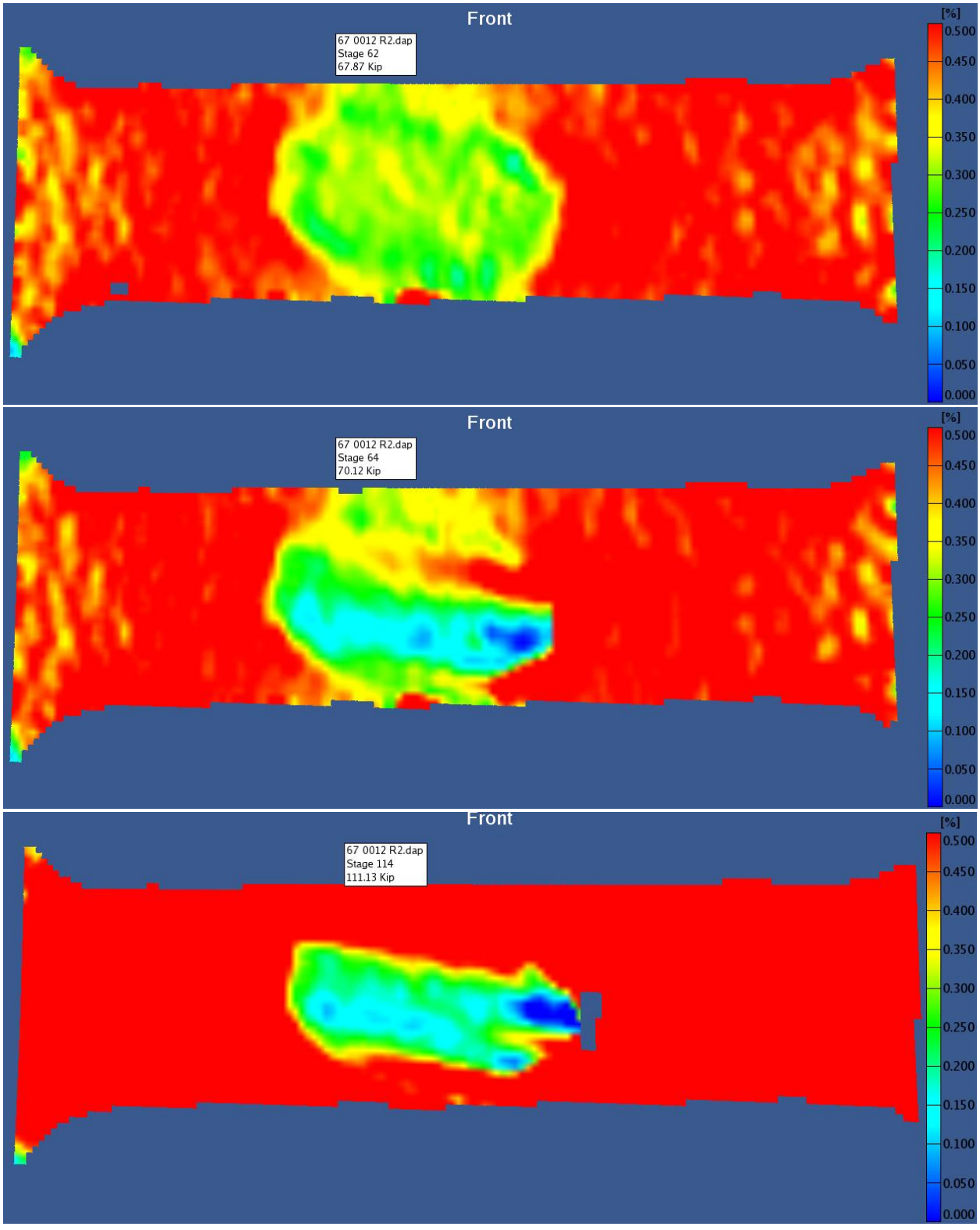

Figure 29. OML Patch Failure Delamination: Repair 67-0012 R 2.

Repair number 66-0158 R 2 had a square edge, aligned OML patch (TI repair) that began to appeared to become disbonded from the substrate at approximately 50 ksi. The load dropped simultaneously with the disbond event, indicating that at least some of the load carried by the patch was released. The load dropped approximately 3,800 lbs (to a stress of approximately 47 ksi). The specimen continued loading from that point to the ultimate stress of 84.2 ksi. Figure 30 shows a progression of SO results displaying the patch strain field prior to the disbond event, after the disbond event, and at the ultimate load of the specimen. Note the patch is "cold" after the disbond event, indicating little to no strain being carried through the patch. The area to the right of the patch appears to be at high strain, but this is actually a large crack in the sealant that the SO system is incorrectly interpreting as high strain (speckles displaced farther apart than surrounding speckles). The OML patch became completely disbonded upon substrate failure and separated from the specimen (reference #AFRL/MLS 06-091).

Specimen number 66-0146 R 1 had a square edge (with rounded corners), aligned OML patch (Lockheed repair) that began to delaminate at both edges of the patch at approximately 73 ksi. One of the delaminations grew under the skin of the specimen, parallel to the edge, with increasing load. The specimen failed at 87.2 ksi. Figure 31 shows the strain field of the patch failure at first detectable occurrence as well as the final maximum extent of the delamination, just prior to substrate failure. Note that the scale used in the figure has been reduced to more clearly show the patch failure.

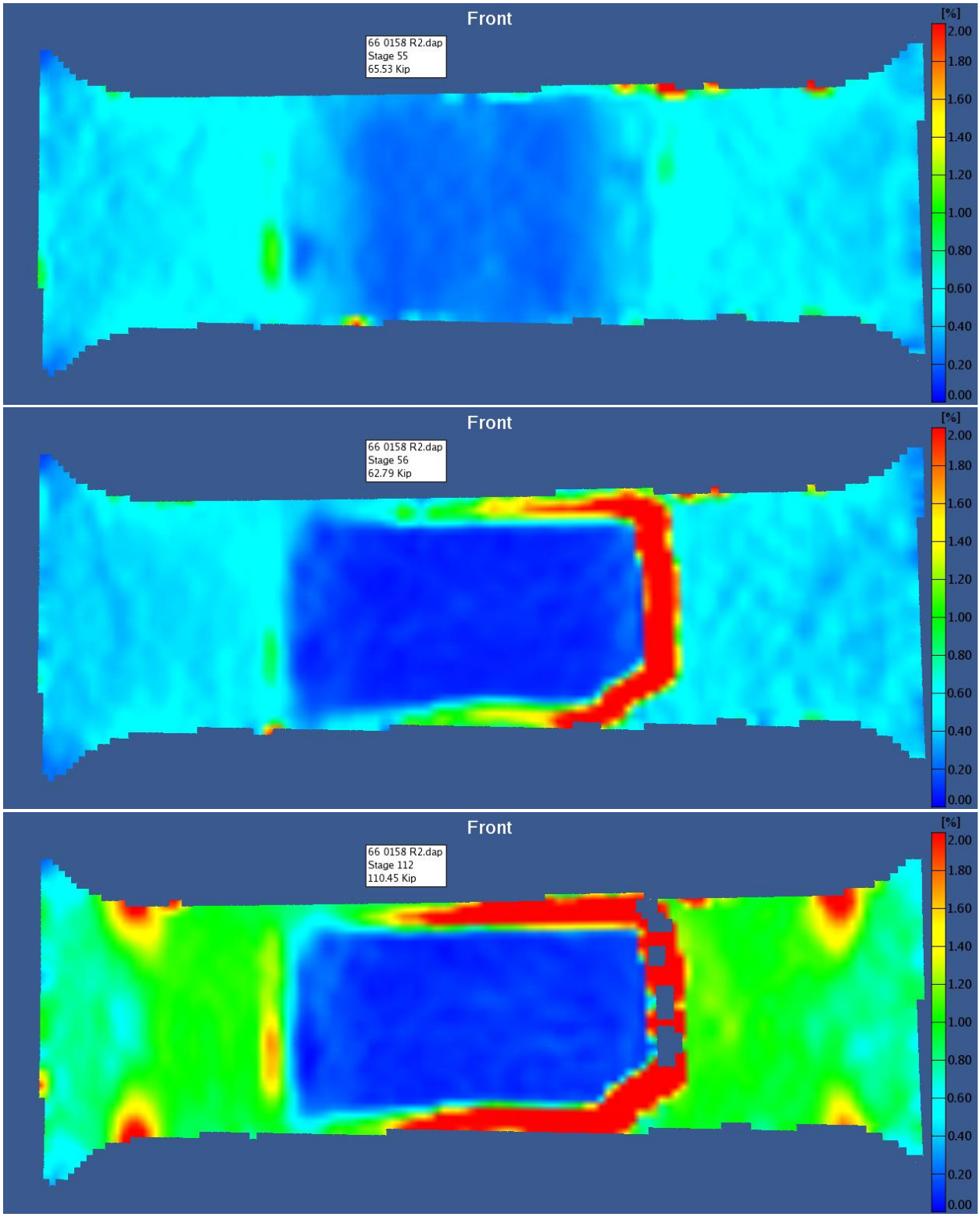

Figure 30. OML Patch Failure Disbond; Repair 66-0158 R 2.

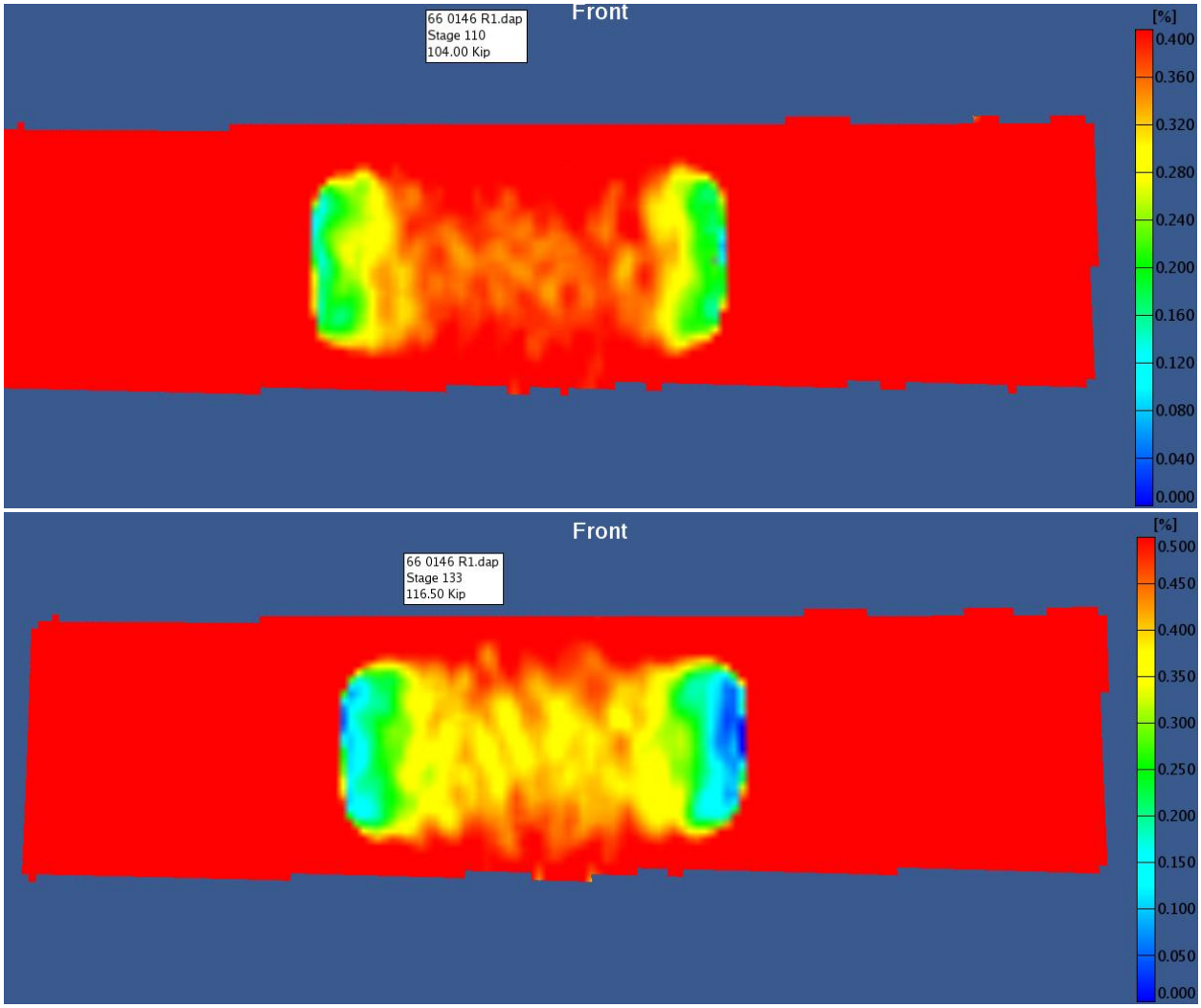

Figure 31. OML Patch Failure Delamination; Repair 66-0146 R 1.

Specimen number 65-0276 R 1 had a clipped edge, aligned OML patch (TI repair) that began to delaminate at both edges of the patch at approximately 77 ksi. One of the delaminations grew under the skin of the specimen, parallel to the edge, with increasing load. The specimen failed at 87.2 ksi. Figure 32 shows the strain field of the patch failure at first detectable occurrence as well as the final maximum extent of the delamination, just prior to substrate failure. Note that the scale used in the figure has been reduced to more clearly show the patch failure.

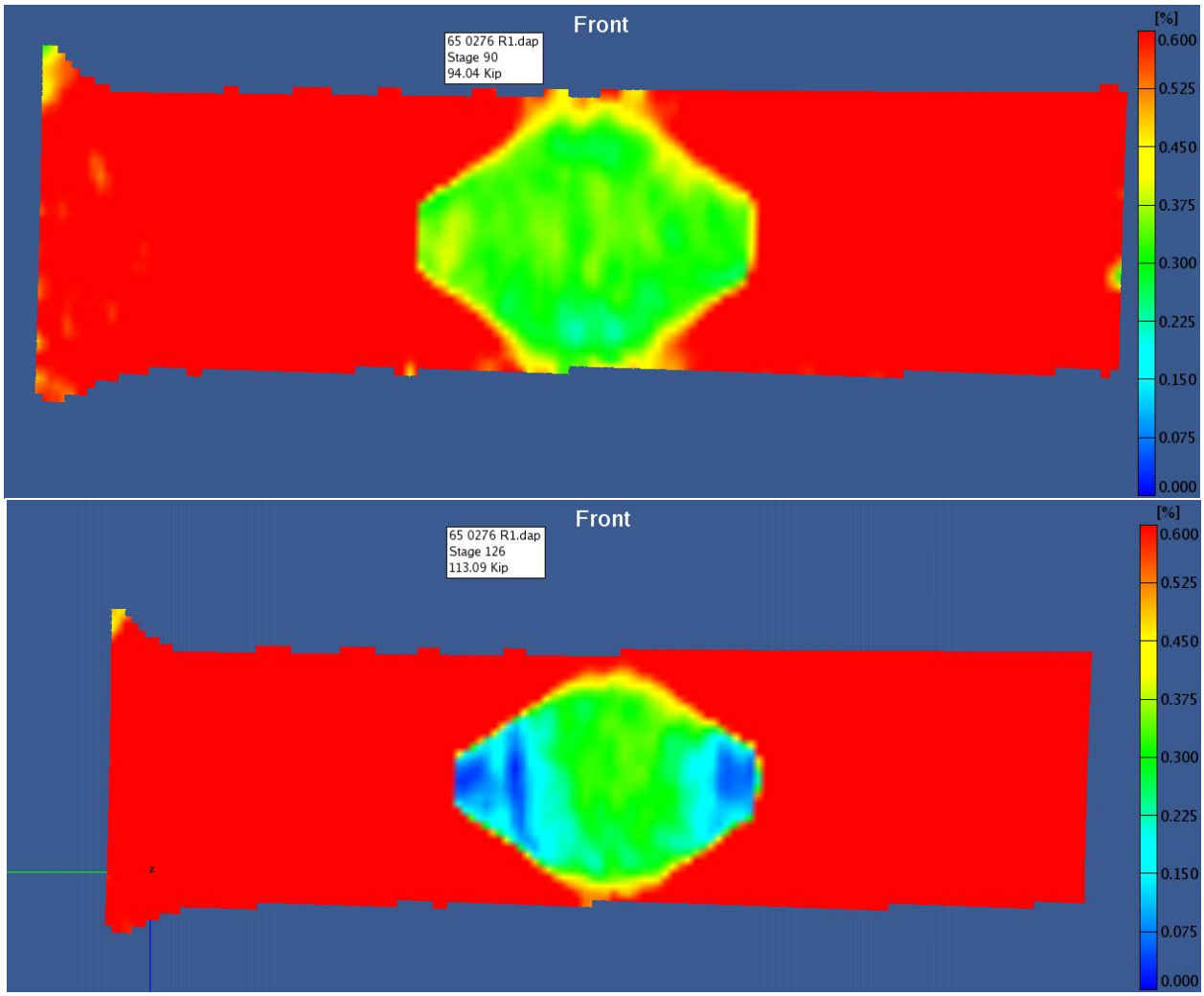

Figure 32. OML Patch Failure Delamination; Repair 65-0276 R 1.

3.2 RESULTS OF NEW REPAIRS

The tabulated results of the residual strength testing on the new repair specimens are presented in Table 7. All of the specimens in this group were original uncracked wing planks that were extracted from areas of the aircraft close to an original repair for baseline material purposes. These planks were machined into specimens of 18-inch gage length. The weep holes were then precracked to the final crack lengths noted in the table. The repairs were based on common repair configurations, with the specific patch design details provided by archived data at Warner-Robins AFB. The patches were bonded with the original surface prep and bonding procedures and materials. The average residual strength of the new repair specimens, using nominal stress data, with no unrepaired weep holes in the gage section was 82.95 ksi. Figures 33 through 36 display the surface strain field of each specimen at the maximum load.

Table 7. Summary of New Repair Residual Strength Data

Test Number	Specimen (Repair) Number	Test Date	Max Load (lbf)	Max Nominal Stress (psi)	Failure Location	Comments
66	66-0196 R 5 P	6/28/2006	110248	83923	Rib Clip Hole	actual crack length 0.257
67	66-7955 R 2 P	6/29/2006	109882	82444	Rib Clip Hole	actual crack length 0.250
68	64-0612 R 1 P	6/28/2006	109552	80907	Rib Clip Hole	actual crack length 0.250
69	64-0628 R 1 P	6/29/2006	117139	84507	Rib Clip Hole	actual crack length 0.785

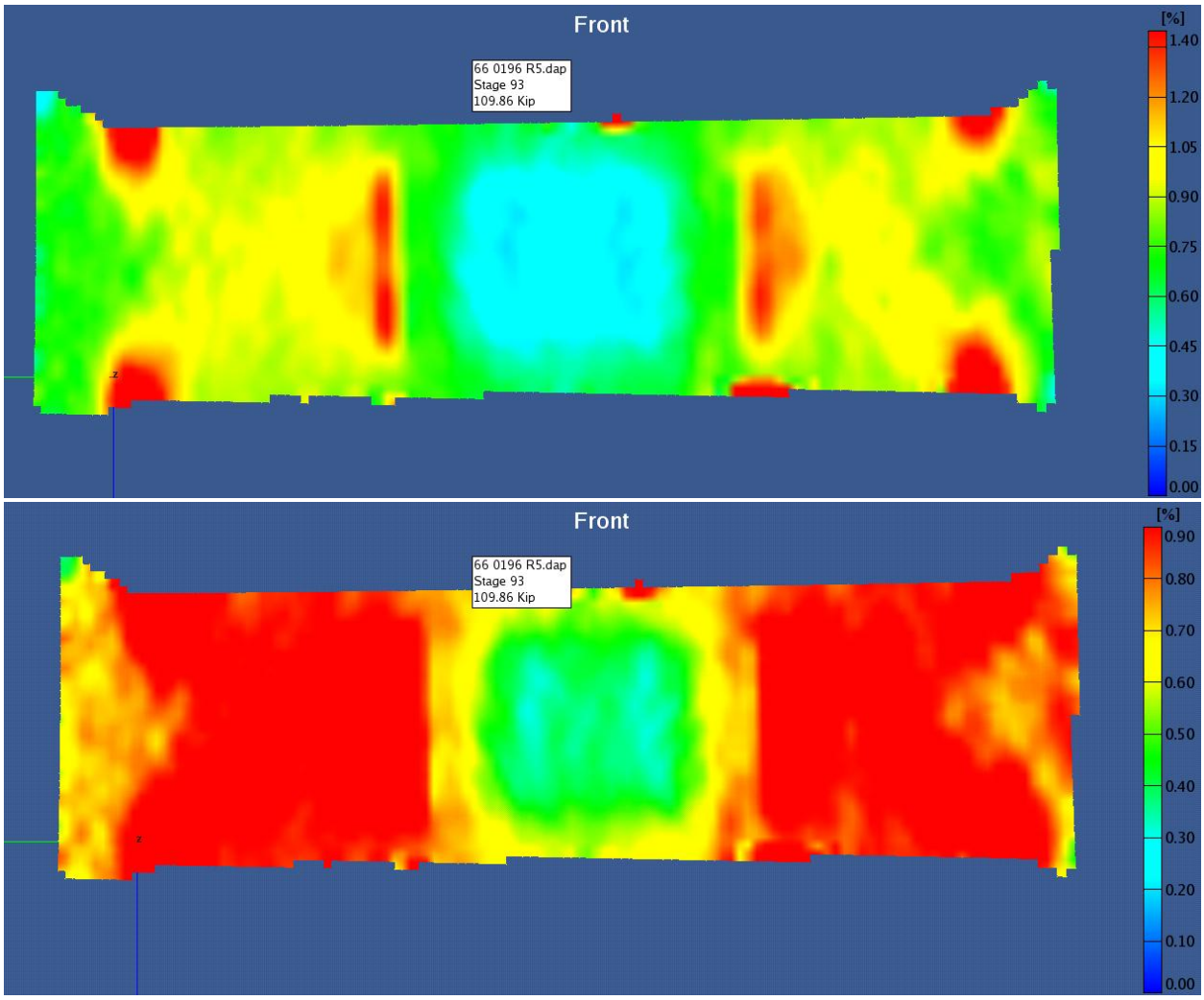

Figure 33. Strain Field of New Repair 66-0196 R 5 P; High scale (top) and Low Scale (bottom) at Ultimate Load.

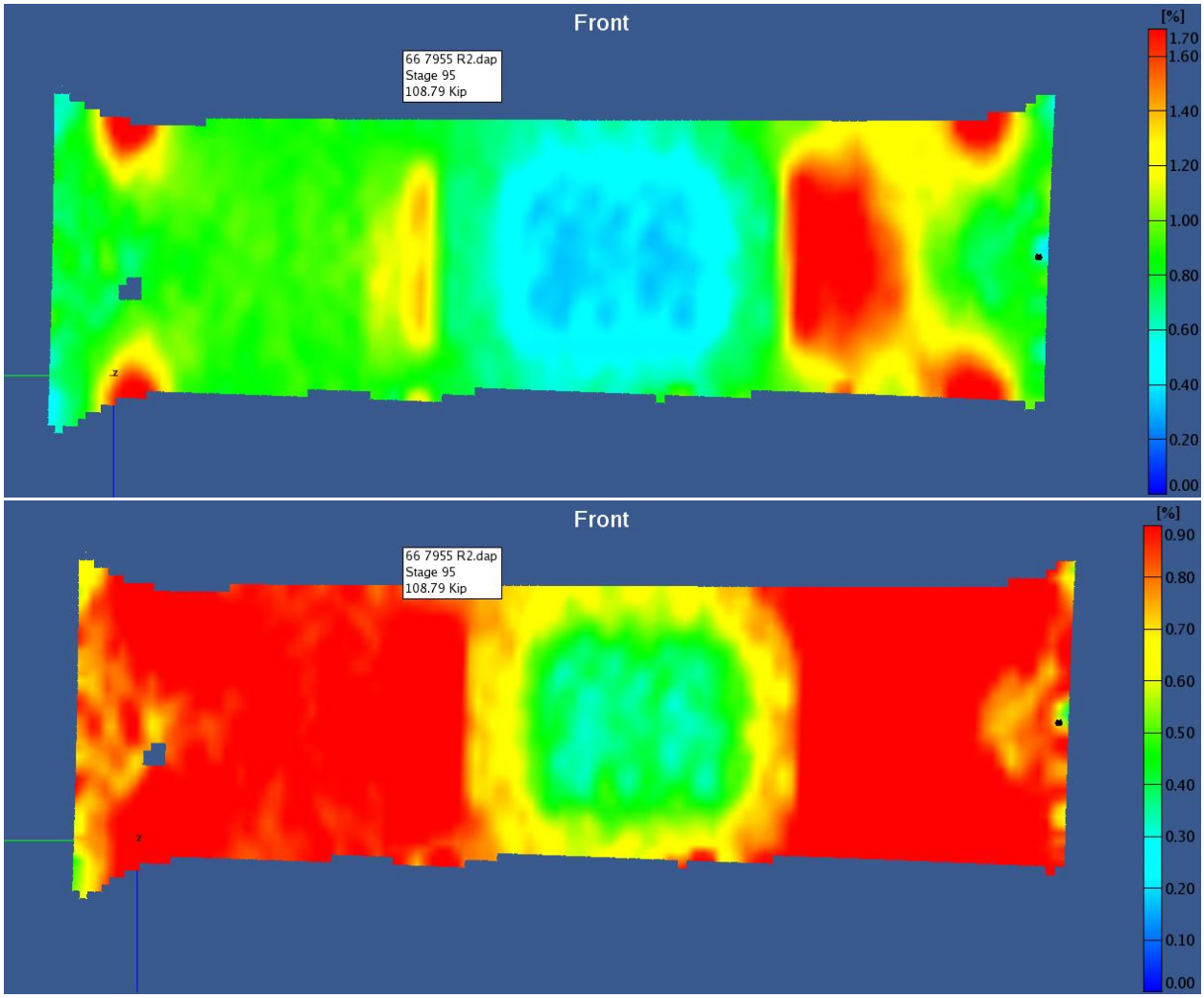

Figure 34. Strain Field of New Repair 66-7955 R 2 P; High Scale (top) and Low Scale (bottom) at Ultimate Load.

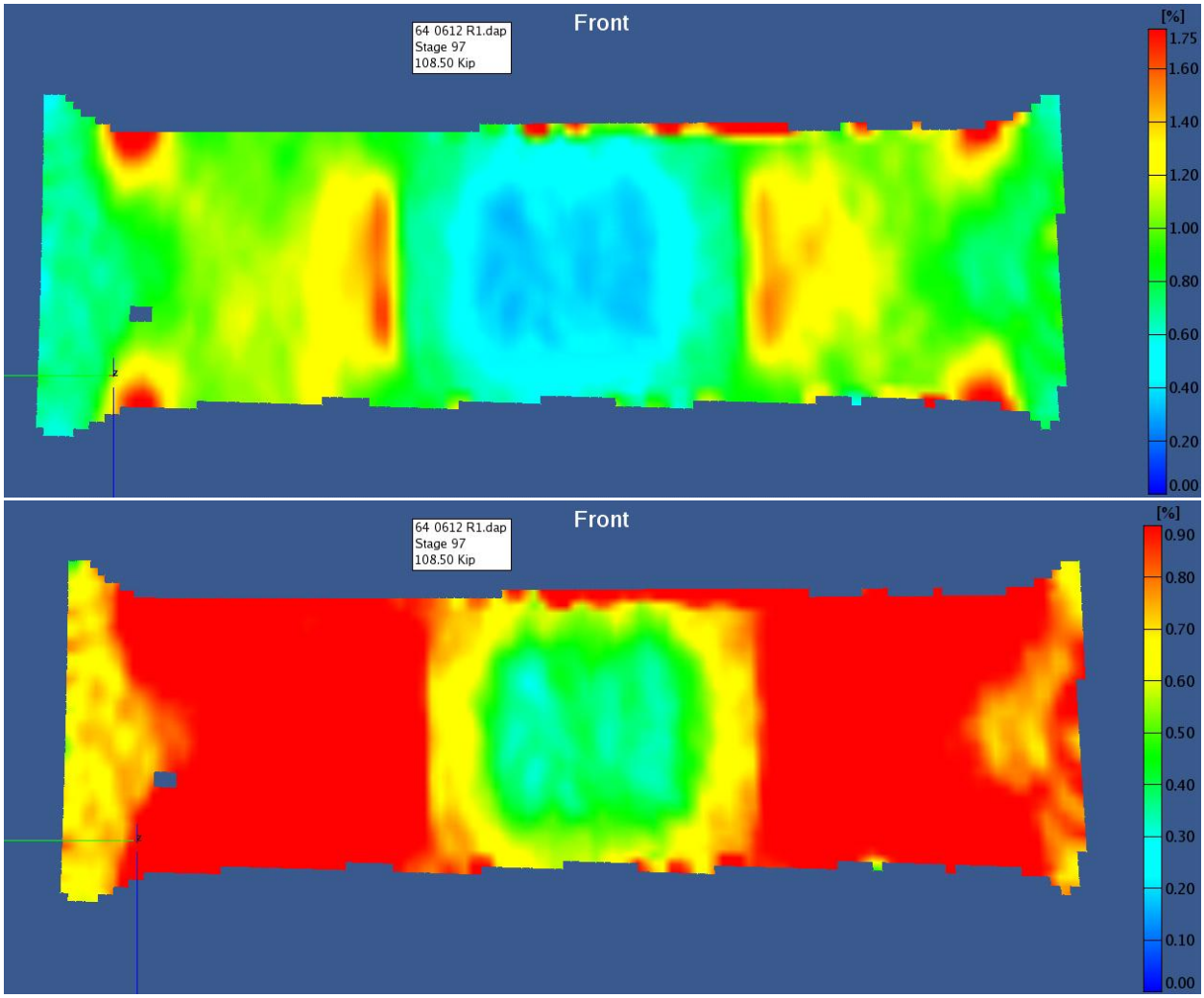

Figure 35. Strain Field of New Repair 64-0612 R 1 P; High Scale (top) and Low Scale (bottom) at Ultimate Load.

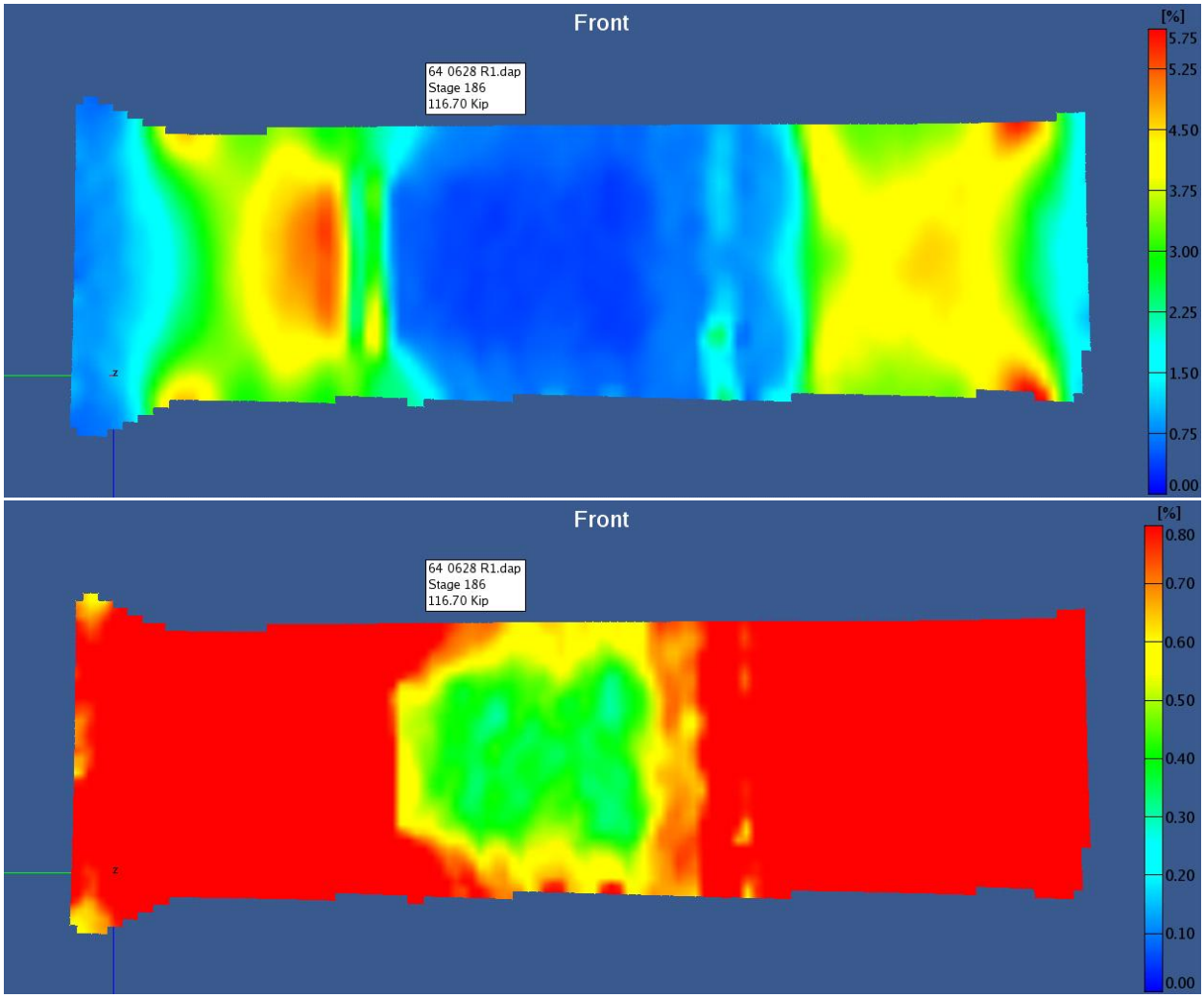

Figure 36. Strain Field of New Repair 64-0628 R 1 P; High Scale (top) and Low Scale (bottom) at Ultimate Load.

3.3 RESULTS OF BASELINE SHARP CRACK SPECIMENS

The tabulated results of the residual strength testing on the baseline cracked residual strength specimens are presented in Tables 8 and 9. Table 8 covers the two original repairs that were selected for baseline testing. These specimens were stripped of the repair patches and tested as if no repair was performed. After the tests were performed, the repaired weep hole section was examined to measure the original crack length. In the case of 67-0021 R 6, the original crack was not found. Table 9 covers the residual strength specimens that were cut from pristine original planks and artificially precracked to the crack length listed in the table.

Table 8. Summary of Sharp Crack Data – Original Repairs (Patches Stripped)

Test Number	Specimen (Repair) Number	Test Date	Max Load (lbf)	Max Nominal Stress (psi)	Failure Location
55	66-0148 R 2	6/13/2006	90826	69397	0.375 inch upcracked weephole
56	67-0021 R 6	6/14/2006	109436	83771	weephole (no original crack found)

Table 9. Summary of Sharp Crack Data – New Cracks

Test Number	Specimen (Repair) Number	Test Date	Max Load (lbf)	Max Nominal Stress (psi)	Failure Location
57	65-0244 R 2 P	6/23/2006	92999	69598	0.254 inch upcracked weephole
58	67-UNKN R 6 P	6/23/2006	74701	57233	0.511 inch upcracked weephole
59	65-0276 R 1 A P	6/26/2006	92303	67077	0.256 inch upcracked weephole
60	66-0153 R 1 P	6/26/2006	93872	70152	0.252 inch upcracked weephole
61	67-0029 R 6 P	**	**	**	broke in precracking
62	65-0276 R 1 B P	6/27/2006	76263	57863	0.375 inch upcracked weephole
63	66-UNKN R 8 P	6/27/2006	76215	55701	0.504 inch upcracked weephole
64	66-0151 R 1 P	**	**	**	broke in precracking
65	66-0136 R 5 P	6/28/2006	77679	59680	0.402 inch upcracked weephole

** - specimen broke during precracking

SECTION 4
CONCLUSIONS

As noted previously, not all test groups contain a sufficient number of specimens to generate statistically based conclusions. The following conclusions are therefore offered solely based on general observations, and should not be construed to be statistically based or influenced.

4.1 ORIGINAL REPAIRS

The majority of original repairs performed on cracked weep holes experienced no patch failures. A few specific repairs did experience a delamination or disbond type of patch failure event in the OML patch. Typically, these failures occurred at very high stress levels, near or beyond the yield stress of the base material. In all cases of a patch delamination or disbond, the riser patches continued to attract and carry load up to specimen failure.

4.2 ORIGINAL REPAIRS VS. NEW REPAIRS

The average nominal residual strength for the group of original repairs and the group of new repairs is similar. The new repairs had an average nominal residual strength of 82.9 ksi, while the original repairs had an average nominal residual strength of 83.2 ksi. The average residual strength values indicate there is little detrimental effect of flight time and environmental degradation that could be detected by residual strength testing.

4.3 LONG CRACK NEW REPAIR

The results of a single new repair (bonded and tested using all of the same procedures and NDI evaluations as the rest of the new repairs) containing an extremely long crack did not show any signs of high (or higher than normal) strain in the crack area, nor did any of the patches fail through the crack section. Of any of the repaired specimens, including original or new repairs, this specimen serves to provide significant confidence in the strength of the repair and the load carrying capability of the repair/adhesive/surface preparation.

4.4 RESIDUAL STRENGTH OF CRACKED UNREPAIRED PANELS

The unrepaired cracked panels provide a good indication of the lower bound for residual strength of the wing skin structure. Although no statistically based conclusions can be drawn, it appears that while the shorter crack lengths have little effect on residual strength, the longer

and unrepaired cracks have significantly detrimental effects. Again, these tests were performed to provide a worst case scenario baseline to compare with any repair that failed through the crack section.

4.5 RISER PATCHES

The riser patches (in doubler configuration) did not fail in a detectable way on any specimen. Results from the SO system gave no indications of delamination or disbonding, nor was any evidence witnessed that indicated the loss of load attraction to the patches. In no cases did the strain gaged riser patches provide any indication of patch failure. In all specimens that experienced an OML patch failure event, the riser patches were studied extensively for load loss, delamination or disbond, unusual strain levels at the weep hole, etc. There was not a single case indicating any sort of patch failure or unexpected behavior in the riser patches.

4.6 STEREO-OPTIC SYSTEM

The use of the Stereo-Optic system in this program proved invaluable to the success of the program. The SO system provided a means to monitor the entire surface of the patch, as well as the visible aluminum substrate surrounding the patch. This allowed the characterization of patch loading and load attraction behavior that would be unavailable by any other method. Although only surface strain could be monitored, the ability of the SO system to monitor strain around the patch helped determine that the delamination observed in one case was an outer ply delamination, and the majority of the patch continued to attract load from the surrounding aluminum and carry the load. The use of strain gages alone would not have detected this unless the gage placement was perfect.